FABRICATION OF ALUMINIUM SURFACE COMPOSITE WITH FRICTION STIR PROCESSING (FSP) AND ITS CHARACTERIZATION

A THESIS SUBMITTED IN PARTIAL FULFILLMENT OF THE REQUIREMENT FOR AWARD OF THE DEGREE OF

MASTER OF TECHNOLOGY

IN

PRODUCTION AND INDUSTRIAL ENGINEERING

SUBMITTED BY

VIKRAM SINGH RAJPUT

ROLL NO.- 2K14/PIE/018

UNDER THE GUIDANCE OF

DR. M. S. NIRANJAN

ASSISTANT PROFESSOR

DELHI TECHNOLOGICAL UNIVERSITY

DEPARTMENT OF MECHANICAL, PRODUCTION & INDUSTRIAL AND AUTOMOBILE ENGINEERING

DELHI TECHNOLOGICAL UNIVERSITY

BAWANA ROAD, DELHI-110042

JULY, 2016

DELHI TECHNOLOGICAL UNIVERSITY

(Formerly Delhi College of Engineering)

Shahbad Daulatpur, Bawana Road,

Delhi-110042

STUDENT'S DECLARATION

I, **Vikram Singh Rajput,** hereby certify that the work which is being presented in this thesis entitled **"Fabrication of Aluminium Surface Composite with Friction Stir Processing (FSP) and its characterization"** is submitted in the partial fulfillment of the requirement for degree of **Master of Technology (Production and Industrial Engineering)** in Department of Mechanical Engineering at **Delhi Technological University** is an authentic record of my own work carried out under the supervision of **Dr. M S Niranjan Assistant Professor, Mechanical Engineering Department, DTU.** The matter presented in this thesis has not been submitted in any other University/Institute for the award of Master of Technology Degree. Also, it has not been directly copied from any source without giving its proper reference.

(Signature of Student)
Vikram Singh Rajput
2K14/PIE/018

DELHI TECHNOLOGICAL UNIVERSITY

(Formerly Delhi College of Engineering)

Shahbad Daulatpur, Bawana Road,

Delhi-110042

CERTIFICATE

This is to certify that the thesis report entitled, **"Fabrication of Aluminium Surface Composite with Friction Stir Processing (FSP) and its characterization"** being submitted by **Vikram Singh Rajput (Roll No. 2K14/PIE/18)** at Delhi Technological University, Delhi for the award of Degree of Master of Technology as per academic curriculum. It is a record of bonafied research work carried out by the student under my supervision and guidance, towards partial fulfillment of the requirement for the award of Master of Technology degree in Production and Industrial Engineering. The work is original as it has not been submitted earlier in part or full for any purpose before.

.

Dr. M. S. Niranjan

Assistant Professor

Mechanical Engineering Department

Delhi Technological University

Delhi-110042

ACKNOWLEDGEMENT

First and foremost, praises and thanks to the God, the Almighty, for his showers of blessings throughout my research work to complete the research successfully.

I would like to extend my gratitude to **Prof. R. S. Mishra, Head,** Department of Mechanical Engineering, Delhi Technological University, for providing this opportunity to carry out the present thesis work.

The constant guidance and encouragement received from **Mr. V. Jaganathan Arulmoni, Associate Professor,** Department of Mechanical Engineering, Delhi Technological University, has been of great help in carrying out the present work and is acknowledge with reverential thanks.

I would like to express my deep and sincere gratitude to my research supervisor, **Dr. M. S. Niranjan, Assistant Professor** Department of Mechanical Engineering, Delhi Technological University, for giving me the opportunity to do research and providing invaluable guidance throughout the research work. His dynamism, vision, sincerity and motivation have deeply inspired me. He has taught me the methodology to carry out the research and to present the research works as clearly as possible. It was a great privilege and honor to work and study under his guidance. I am extremely grateful for what he has offered me. I would also like to thank him for his friendship, empathy, and great sense of humor. Without the wise advice and able guidance, it would have been impossible to complete the thesis in this manner.

I would like to offer my enduring gratitude to **Dr. Ranganath M. S., Associate Professor** and **Mr. K Srinivas, Assistant Professor**, Department of Mechanical Engineering, Delhi Technological University who regularly motivated me as well as other faculty, staff and our fellow students at the DTU, who have inspired us to continue our work in this field.

I am extremely grateful to my parents and family for their love, prayers, caring and sacrifices for educating and preparing me for my future.

VIKRAM SINGH RAJPUT
M.Tech (PRODUCTION AND INDUSTRIAL ENGINEERING)
2K14/PIE/018

ABSTRACT

Now a days, fabrication of metal matrix composites (MMCs) with improved mechanical properties and modified microstructures has attracted many attentions. One of the methods to produce MMCs is friction stir processing (FSP) which is a novel modifying technique. FSP is a method of changing the properties of metal through intense, localized plastic deformation. This deformation is produced by forcibly inserting a non-consumable tool into the work-piece, and revolving the tool in a stirring motion as it is pushed laterally through the work-piece. It comprises of a rotating tool with pin and shoulder which are inserted into a single piece of material and traversed along the desired path to cover the region of interest. Friction between the shoulder and work piece results in localized heating which raises the temperature of the material to the range where it is plastically deformed. During this process, severe plastic deformation occurs and due to thermal exposure of material, it results in a significant evolution in the local microstructure.

The present work aims the fabrication of AA6061-T6 surface composite with reinforced layers of boron carbide (B_4C), Silicon Carbide (SiC) and mixture of both through FSP. Micro-structural characterization are performed through optical microscopy (OM) and scanning electron microscope (SEM). The effects of different reinforced particles are investigated on microstructure and micro hardness. Mechanical property such as tensile strength of specimen has been evaluated with and without reinforced particles by using friction stir processing. The tribological behavior such as wear on surface has been observed with Pin on Disc Tribometer.

It has been observed that the micro hardness as well as hardness, wear rate and tensile strength of the MMC's are found better by reinforcement with Boron Carbide during FSP.

Keywords: MMC's, FSP, B_4C, SiC, OM, SEM, Wear.

CONTENTS

LIST OF FIGURES

LIST OF TABLES

LIST OF SYMBOLS

B_4C	Boron Carbide
SiC	Silicon Carbide
℃	deg C
g/cm^3	density unit (gram per cubic centimetre)
hrs	hours(unit of time)
e.g.	For Example
/K	Thermal expansion unit (per degree Kelvin)
MPa	Mega Pascal
Max.	Maximum
W/mK	Watt per metre Kelvin (conductivity)
Ωm	Ohm metre(resistivity unit)
HB	Brinell Hardness
Hv	Vickers hardness
mm	Millimetre
=	Equal to
i.e.	That is
&	And
v/v	Volume by Volume
w/w	Weight by Weight

LIST OF ABBREVIATIONS

Al	Aluminium
AA	Aluminium Alloy
HIP	Hot isostatic pressing
DXZ	Dynamically Recrystallized Zone
ARBed	Accumulative roll bonding
FSPed	Friction Stir Processed
TWI	The Welding Institute
ECAE	Equal Channel Angular Extrusion
FSP	Friction Stir Processing
SCL	Surface Composite Layer
HAZ	Heat affected zone
NZ	Nugget Zone
SEM	Scanning Electron Microscopy
TMAZ	Thermo mechanically affected zone
TEM	Transmission electron microscope

Chapter 1 INTRODUCTION

1.1 Significance of Friction Stir Processing

Selection of material with specific properties is one of the key parameter in many industrial applications, especially in the field of aircraft, shipping and automotive industries. However, processing of such alloys with specific properties, like high strength, suffers due to high cost and time of production, apart from the reduction in ductility. High strength in addition with high ductility is possible with materials having fine and homogenous grain structures. Hence, there arises a necessity to develop a processing technique that would produce a material with small grain size that fulfills the requirements of strength and ductility as well as the cost and time of production. There are some new processing techniques like Equal Channel Angular Extrusion (ECAE), Friction Stir Processing (FSP), being developed for this purpose.

FSP expands the innovation of friction stir welding (FSW) developed by "The Welding Institute (TWI)" of United Kingdom in 1991 to develop local and surface properties at selected locations. FSP is a unique and new thermomechanical processing technique that alters the mechanical and microstructural properties of the material in a single or multiple pass to achieve maximum performance with low production cost in less time.

In the present scenario, FSP is investigated as a potential processing technique for aluminium, copper, and magnesium alloys because of various advantages it offers over Equal Channel Angular Extrusion (ECAE). One of the unique potential application of FSP is in superplastic forming (SPF), which is a net shape forming technique. Super plasticity is a phenomenon exhibited by fine-grained material during which all these materials exhibit an elongation of more than 200% under controlled conditions.

FSP offers many advantages over conventional and also the newer techniques of material processing which include being a single step process, use of the simple and inexpensive tool, less processing time, use of existing and readily available machine tool technology, adaptability to robot use, suitability to automation, being energy efficient and environmental friendly. Though, the limitations of FSP are being reduced by intensive research and development, it still has few limitations that include the rigid clamping of work pieces, backing plate requirement, and the keyhole at the end of each pass. These above mentioned features of the FSP make it a potential

processing technique not only of the aluminum alloys for various industrial applications especially for the SPF but also in the fields of surface engineering, like metal-matrix composite production.

1.2 Principle of FSP

The schematic of FSP is shown in fig. 1.1. To process the sheet by friction stir, a specially designed cylindrical tool in rotary condition is used which is plunged into the selected area. The tool has a small diameter pin with the concentric larger diameter shoulder. When the tool is plunged into the sheet, the rotating pin contacts the surface and friction between the sheet surface and the shoulder rapidly heats and softens a small column of metal, enabling the transverse movement of the tool through the material. The tool shoulder and length of the probe control the depth of penetration.

During FSP, the area to be processed and the tool are moved relative to each other such that the tool traverses, with the overlapping passes, until all the entire selected area is processed to a desired (fine) grain size. The processed zone cools as the tool passes, forming a defect free, and dynamically recrystallized equiaxed fine-grained microstructure.

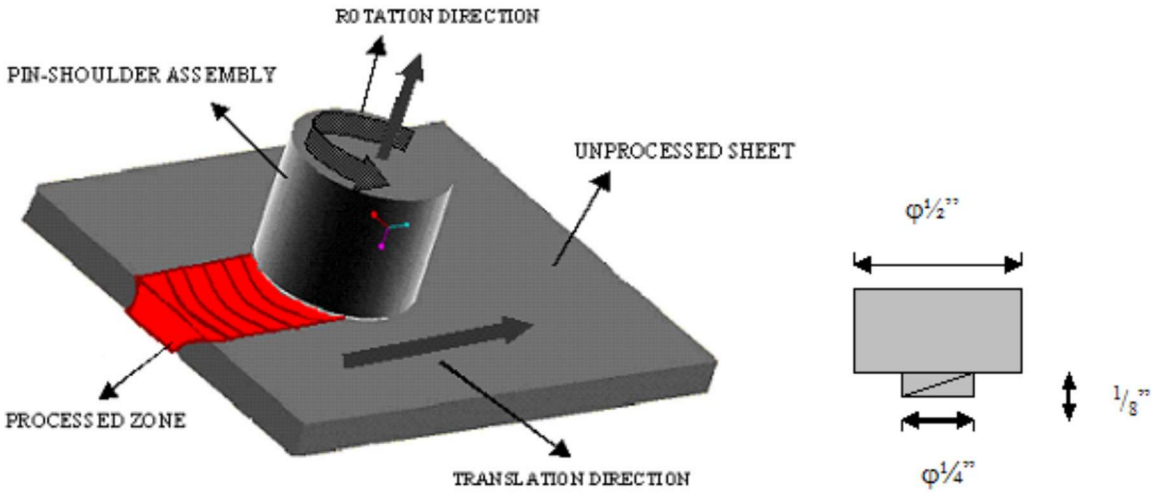

Fig. 1.1: Schematic of friction stir process

1.3 Current research in the field of FSP

As FSP is a relatively new process, researchers are not only investigating the possible aluminum alloys that can be processed but they are also looking into effects of process parameters on various microstructural and mechanical properties. This process can easily be adopted as a processing technique to obtain finer grains.

Extensive studies are carried out in FSP in order to make it cost effective in the automotive and aerospace industries. Many researchers have taken up the microstructural investigation of various friction stir welded and processed aluminum alloys [7-13]. They basically investigated the grain refinement in the processed and the heat affected zones and it has been observed that the FSP of commercially available Al alloys with series 1100, 2024, 5083, 6061, 7075 and 7475 result a significant enhancement in superplastic properties. Different material properties like microstructure, tensile strength, fatigue and hardness are also being examined for different alloys of aluminum. The efforts have been made to investigate the effect of various process parameters like rotational speed, no. of passes, axial load etc. on the properties and microstructure evolved during FSP.

As the concept of FSP is relatively new, and there are many areas, which need thorough investigation to optimize and make it commercially viable. In order to obtain the desired finer grain size, certain process parameters, like translation and rotational speeds, tool geometry etc., are to be controlled. Several investigations are being carried out in order to study the effects of these process parameters on the grain structure. The chemical composition and mechanical properties of different aluminium alloy are given below in table 1.1 and 1.2 respectively.

Table 1.1: Chemical composition for aluminium alloy 6082 and 6061 (by wt.) [17]

Element	AA 6082	AA6061
Si	0.7-1.3	0.4-0.8
Fe	0.0-0.5	Max 0.7
Cu	0.0-0.1	0.15-0.40
Mn	0.4-1.0	max 0.15
Mg	0.6-1.2	0.8-1.2
Zn	0.0-0.2	max.0.25
Ti	0.0-0.1	max. 0.15
Cr	0.0-0.25	0.04-0.35
Al	Balance	Balance

Table 1.2: Mechanical properties of selected aluminium alloys. [17]

Alloy	Temper	Proof Stress 0.20% (MPa)	Tensile Strength (MPa)	Shear Strength (MPa)	Elongation A5 (%)	Elongation A50 (%)	Hardness Brinell HB	Hardness Vickers HV	Fatigue Endur. Limit (MPa)
AA1050A	H2	85	100	60	12		30	30	
	H4	105	115	70	10	9	35	36	70
	H6	120	130	80	7		39		
	H8	140	150	85	6	5	43	44	100
	H9	170	180			3	48	51	
	0	35	80	50	42	38	21	20	50
AA2011	T3	290	365	220	15	15	95	100	250
	T4	270	350	210	18	18	90	95	250
	T6	300	395	235	12	12	110	115	250
	T8	315	420	250	13	12	115	120	250
AA3103	H2	115	135	80	11	11	40	40	
	H4	140	155	90	9	9	45	46	130
	H6	160	175	100	8	6	50	50	
	H8	180	200	110	6	6	55	55	150
	H9	210	240	125	4	3	65	70	
	0	45	105	70	29	25	29	29	100
AA5083	H2	240	330	185	17	16	90	95	280
	H4	275	360	200	16	14	100	105	280
	H6	305	380	210	10	9	105	110	
	H8	335	400	220	9	8	110	115	
	H9	370	420	230	5	5	115	120	
	0	145	300	175	23	22	70	75	250
AA5251	H2	165	210	125	14	14	60	65	
	H4	190	230	135	13	12	65	70	230
	H6	215	255	145	9	8	70	75	
	H8	240	280	155	8	7	80	80	250
	H9	270	310	165	5	4	90	90	
	0	80	180	115	26	25	45	46	200
AA5754	H2	185	245	150	15	14	70	75	
	H4	215	270	160	14	12	75	80	250
	H6	245	290	170	10	9	80	85	
	H8	270	315	180	9	8	90	90	280
	H9	300	340	190	5	4	95	100	
	0	100	215	140	25	24	55	55	220
AA6061	0	50	100	70	27	26	25	85	110
	T1	90	150	95	26	24	45	45	150
	T4	90	160	110	21	21	50	50	150

	T5	175	215	135	14	13	60	65	150
	T6	210	245	150	14	12	75	80	150
	T8	240	260	155		9	80	85	
AA6082	0	60	130	85	27	26	35	35	120
	T1	170	260	155	24	24	70	75	200
	T4	170	260	170	19	19	70	75	200
	T5	275	325	195	11	11	90	95	210
	T6	310	340	210	11	11	95	100	210
AA6262	T6	240	290		8				
	T9	330	360		3				
AA7075	0	105	225	150		17	60	65	230
	T6	505	570	350	10	10	150	160	300
	T7	435	505	305	13	12	140	150	300

Chapter 2 LITERATURE REVIEW

Friction stir technology is a revolution in the field of welding. This innovative technique produces very fine grains in weld zones. If this could be used as a processing technique, it would replace the existing traditional, complex and expensive processing techniques especially for aluminum alloys. FSP can enhance superplasticity in aluminium alloy.

2.1 General idea of the friction stir technology

This section gives an insight into the innovative technology called friction stir technology. The action of rubbing two objects together causing friction to provide heat is one dating back many centuries as stated by Thomas et al [1]. The principles of this method now form the basis of many traditional and novel friction welding, surfacing and processing techniques. The friction process is an efficient and controllable method of plasticizing a specific area on a material, and thus removing contaminants in preparation for welding, surfacing/cladding or extrusion. The process is environmentally friendly as it does not require consumables (filler wire, flux or gas) and produces no fumes. In friction welding, heat is produced by rubbing components together under load. Once the required temperature and material deformation is reached, the action is terminated and the load is maintained or increased to create a solid phase bond. Friction is ideal for welding dissimilar metals with very different melting temperatures and physical properties. Some of the friction stir technologies are shown in the fig. 2.1.

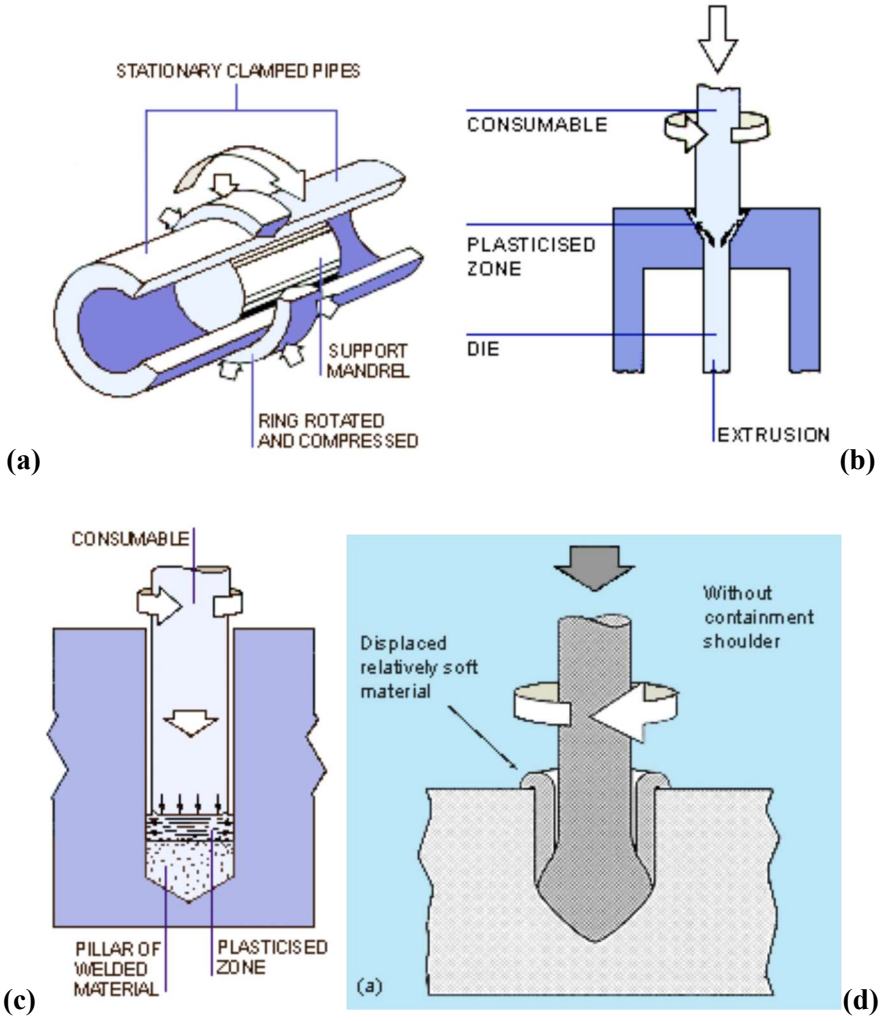

Fig. 2.1: Schematic of a) radial friction welding, b) friction extrusion, c) friction hydro pillar processing d) friction plunge welding without containment shoulder [1]

Work carried out at The Welding Institute (TWI) by Thomas et al [2-3] has demonstrated that several alternative techniques exist or are being developed to meet the requirement for consistent and reliable joining of mass production aluminum alloy vehicle bodies. Three of these techniques (mechanical fasteners, lasers and friction stir welding) are likely to make an impact in industrial processing over the next 5 years. FSW could be applied in the manufacture of straight-line welds in sheet and extrusions as a low cost alternative to arc welding (e.g. in the fabrication of truck floors or walls). The development of robotized friction stir welding heads could extend the range of applications into three dimensional components.

Mishra et al [4] extended the FSW innovation to process Al 7075 and Al 5083 in order to render them superplastic. They observed that the grains obtained were recrystallized, equiaxed

and homogeneous with average grain sizes <5μm. They had high angles of disorientation ranging from 20 degrees to 60 degrees. They had also performed high temperature tensile testing in order to understand the superplastic behavior of FSP aluminum sheets.

Metal matrix composites reinforced with ceramics exhibit high strength, high elastic modulus and improved resistance to wear, creep and fatigue compared to unreinforced metals. Mishra et al [5] experimented and proved that surface composites could be fabricated by friction stir processing. Al/SiC surface composites with different volume fractions of particles were successfully fabricated. The thickness of the surface composite layer ranged from 50 to 200μm. The SiC particles were uniformly distributed in the aluminum matrix. The surface composites have excellent bonding with the aluminum alloy substrate. The micro hardness of the surface composite reinforced with 27 volume % SiC of 0.7 μm average particle size was ~173 Hv, almost double of the 5083Al alloy substrate (85 Hv). The solid-state processing and very fine microstructure that results are also desirable for high performance surface composites.

Thomas et al [6] presented a review of friction technologies for stainless steel, aluminum, and stainless steel to aluminum, which are receiving widespread interest. Friction hydro pillar processing, friction stir welding (FSW), friction plunge welding is some of these unique techniques. They observed that this technology made possible the welding of unweldable aluminum alloys and stainless steel feasible. Using this technology sheets up to 75mm thickness can also be easily welded.

2.2 Microstructural studies on friction stirred alloys

A basic understanding of the evolution of microstructure in the dynamically recrystallized region of FS material and relation with the deformation process variables of strain, strain rate, temperature and process parameters is very essential. This section would give an insight into such studies.

Peel et al [7] reported the results of microstructural, mechanical property and residual stress investigations of four AA5083 FS welds produced under varying conditions. It was found that the weld properties were dominated by the thermal input (thermal excursion) rather than the mechanical deformation by the tool, resulting in more than 30 mm wide zone of equiaxed grains around the weld line. Increasing the traverse speed and hence reducing the heat input narrowed

the weld zone. It is observed that the recrystallization resulting in the weld zone had considerably lower hardness and yield strength than the parent AA5083. In tensile test, almost all the plastic flow occurred within the recrystallized weld zone and the synchrotron residual stress analysis indicated that the weld zone is in tension in both the longitudinal and transverse directions. The peak longitudinal stresses found increased as the traverse speed increases. This increase is probably due to steeper thermal gradients during welding and the reduced time for stress relaxation to occur. The tensile stresses appear to be limited to the softened weld zone resulting in a narrowing of the tensile region (and the peak stresses) as the traverse speed increased. Measurements of the unstrained lattice parameter ($d0$) indicated variations with distance from the weld line that would result in significant errors in the inferred residual stresses if a single value for $d0$ were used for diffraction based experiment.

The evolution of the fine-grained structure in friction-stir processed aluminum has been studied by Rhodes et al [8] using a rotating-tool plunge and extract technique. In these experiments, the rotating tool introduced severe deformation in the starting grain structure, including severe deformation of the pre-existing sub-grains. Extreme surface cooling was used to freeze in the starting structure. Heat generated by the rotating tool was indicated as a function of the rotation speed and the external cooling rate. At slower cooling rates and/or faster tool rotation speeds, recrystallization of the deformed aluminum was observed to occur. Initial sizes of the newly recrystallized grains were found in order of 25–100 nm, considerably smaller than the pre-existing sub-grains in the starting condition. Subsequent experiments revealed that the newly recrystallized grains grow to a size (2–5μm) equivalent to that found in friction-stir processed aluminum, after heating 1–4 min at 350–450 °C. It is postulated that the size of 2–5 μm grains found in friction-stir welded and friction-stir processed aluminum alloys arose as a result of nucleation and growth within a heavily deformed structure and not from the rotation of pre-existing sub grains.

Sato et al [9] applied FSW to an accumulative roll-bonded (ARBed) Al alloy 1100. FSW resulted in reproduction of fine grains in the stir zone and small growth of the ultrafine grains of ARBed material just outside the stir zone. FSW was reported to suppress large reductions of hardness in the ARBed material, although the stir zone and thermo mechanical affected zone (TMAZ) experienced small reductions of hardness due to dynamic recrystallization and

recovery. Consequently, FSW effectively prevented the softening in the ARBed alloy which had an equivalent strain of 4.8.

The microstructure evolution of a joint of Al–Si–Mg alloys A6056-T4 and A6056-T6 was characterized using transmission electron microscopy (TEM) as shown in fig. 2.2 by Cabibbo et al [10]. Metallurgical investigations, hardness and mechanical tests were also performed to correlate the TEM investigations to the mechanical properties of the produced FSW butt joint. After FSW, thermal treatment was carried out at 530 °C followed by ageing at 160 °C (T6). The base material (T4) and the heat-treated one (T6) were put in comparison showing a remarkable ductility reduction of the joint after T6 treatment i.e., it was 80-90% of that of the parent material.

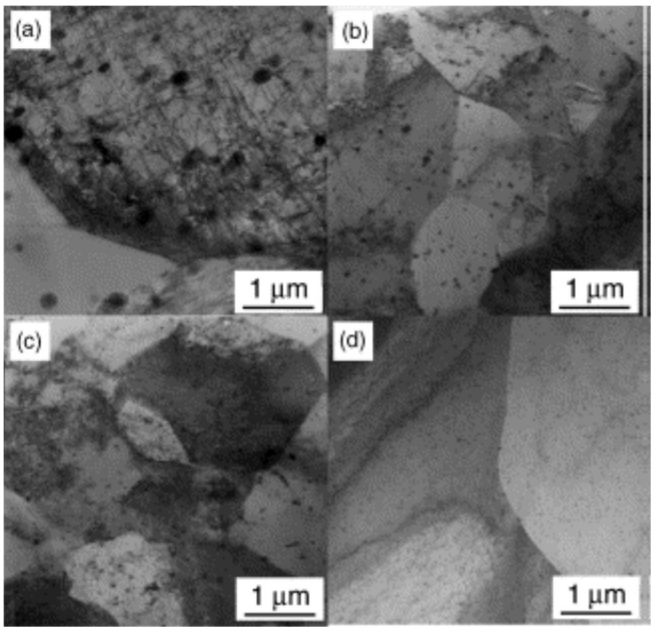

Fig. 2.2: Microstructure of T4-FSW material. (a) Elongated grain zone of the heat-affected region; (b) dynamically recrystallized grains. T4 and T6 microstructure after FSW; dynamically recrystallized zone of T4 (c) and T6 (d). TEM [10]

The microstructure of a FSW Al–6.0Cu–0.75Mg–0.65Ag (wt.%) alloy in the peak-aged T6 temper was characterized by TEM by Lity ska et al [11]. Strengthening precipitates found in the base alloys dissolved in the weld nugget, while it was observed that in the heat-affected zone they were coarsened considerably, causing softening inside the weld region. Precipitates of the Ω (Al2Cu) phase, was considered as the main strengthening phase in base material, grew up to 200– 300 nm in the heat-affected zone, but their density decreased.

The grain structure, dislocation density and second phase particles in various regions including the dynamically recrystallized zone (DXZ), thermo-mechanically affected zone (TMAZ), and heat affected zone (HAZ) of a FSW aluminum alloy 7050-T651 were investigated and compared with the unaffected base metal by Su et al [12] as shown in fig. 2.3 and 2.4 respectively. Frequently, the weld nugget appears to comprise of equiaxed, fine, dynamically recrystallized grains whose size is substantially less than that in the parent material. This feature of friction stirred zone resulted in the development of new economical, energy efficient, thermomechanical material processing technique called FSP. It was performed on aluminum alloys for example 7075 Al and 6061 Al specially to render them superplastic and also has been used as a technique to produce aluminum surface metal matrix composite.

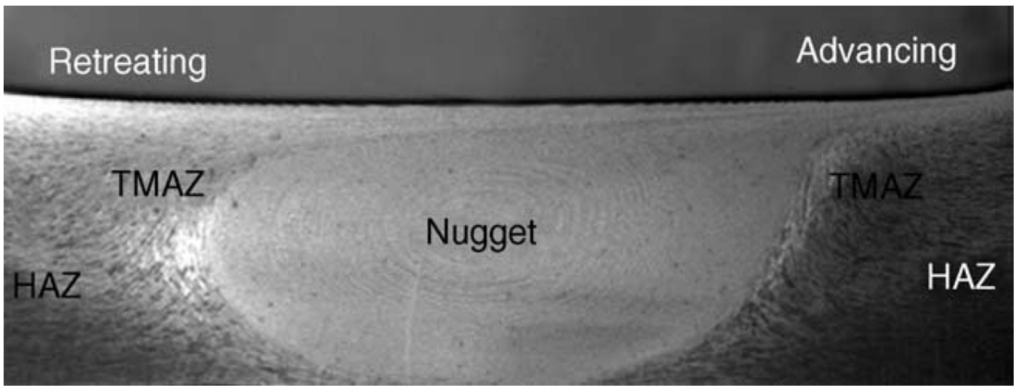

Fig. 2.3: Various zones in the cross-section of FSP AA7075 [12]

The study mainly concentrated on the grain size obtained in the weld zone. There are studies on the temperature distribution over the entire weld zone and its effect on the microstructure. Some studies were specifically concentrating on the precipitation phenomenon and type of precipitants obtained in the welded region. Investigations were made on the effect of rotational speed on microstructure.

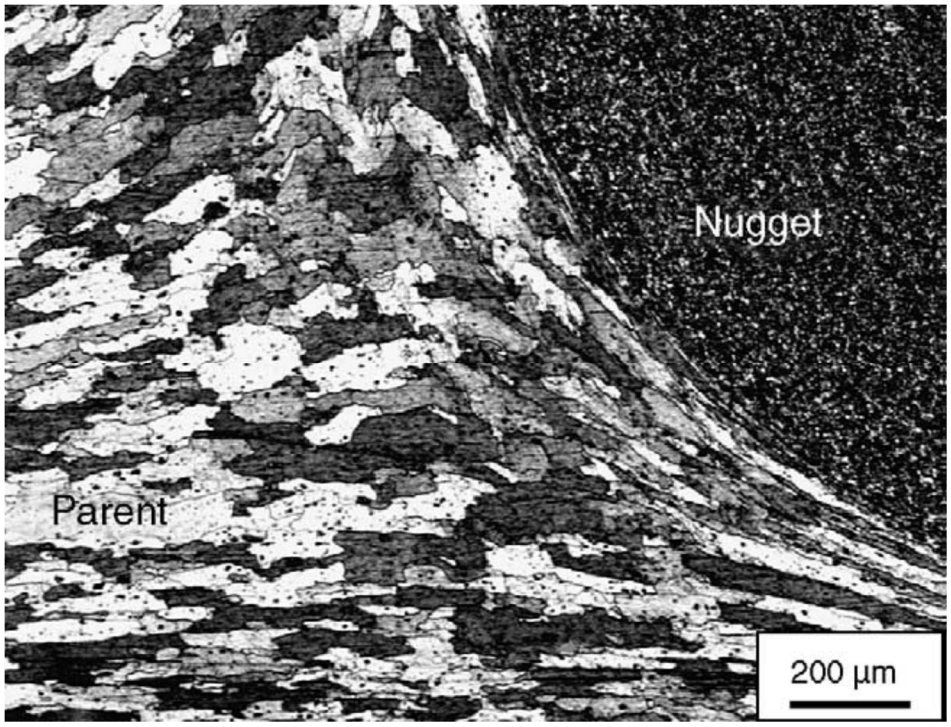

Fig. 2.4: Microstructure of thermo-mechanically affected zone in FSP AA7075 [12]

2.3 Process parameters and properties during FSP

In order to optimize any process, it is very essential to understand the effect of process parameters on the properties of the processed material. Hence, this section gives an overview of such investigation in the field of friction stir welding process.

Kwon et al [13] studied the FS processed Al 1050 alloy. The hardness and tensile strength of the FS processed 1050 aluminum alloy were observed to increase significantly with decreased tool rotation speed. It was noted that, at 560 rpm, these characteristics seemed to increase as a result of grain refinement by up to 37% and 46% respectively compared to the starting material.

Friction stir processing of nanophase aluminum alloys led to high strength ~ 650 MPa with good ductility above 10% as shown in fig. 2.5. Improvements in ductility were due to significantly improved homogenization of microstructure during FSP. The FSP technique is very effective in producing ductile, very high specific strength aluminum alloys, such as Al- Ti-Cu and Al-Ti-Ni as investigated by Beron et al [14]. The authors investigated two processes: hot

isostatic pressing (HIP) and friction stir process (FSP) and then compared the microstructures and corresponding properties resulted from respective processes on 7075 Al alloy. HIP results in a very high strength alloy with low ductility and inhomogeneous structure. But FSP results in comparatively low strength below 740 Mpa but very high ductility at temperatures above 300°C at ~500°C. However, the FS processing parameters can be optimized to lower both the operating temperature and time at the temperature in order to improve the strength further.

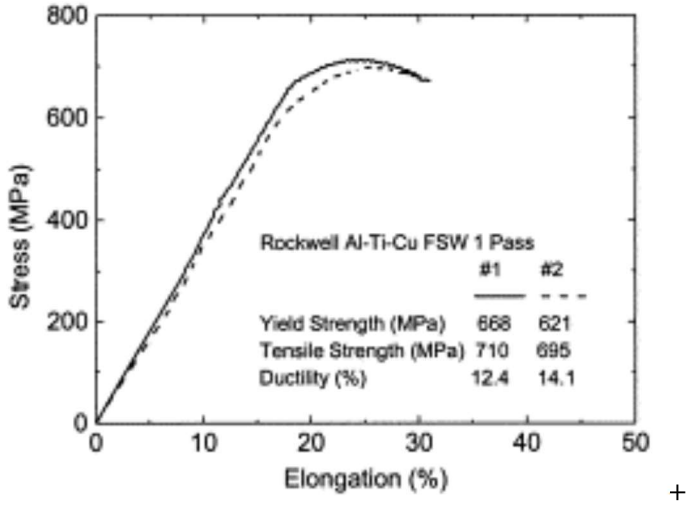

Fig. 2.5: Tensile tests of FS processed material show an excellent strength and more than 10%ductility [14]

Deva et al [15] studied the surface composite hybrid of AA6061-T6 using FSP. He found that Microhardness increases due to presence and pining effect of hard SiC and Al_2O_3 particles. Low wear rate was exhibited in the Al–SiC/Gr surface hybrid composite due to mechanically mixed layer generated between composite pin and steel disk surfaces which contained fractured SiC and Gr. The presence of SiC particles serves as load bearing elements and Gr particles acted as solid lubricant. Tensile properties are decreased as compared to the base material due to the presence of reinforcement particles which make the matrix brittle.

Vipin et al [16] studied the Fabrication of Al5083/B_4C surface composite by friction stir processing and its tribological characterization. They found that the microstructure in the FSPed specimens with nano B_4C particles three passes exhibits fine grain size, higher hardness (124.8 Hv), ultimate strength (360 Mpa) and wear rate (0.00327 mg/m) in comparison to the base material hardness (82 Hv), ultimate strength (310 Mpa) and wear rate (0.0057 mg/m). By increasing the FSP passes, the distribution of nano particles in the Al matrix becomes uniform

which has resulted in increased hardness, in comparison with one pass FSP nano composite. The microhardness of the Al/B_4C surface nano composites is higher in comparison with B_4C micro particles. The presence of nano size B_4C particles contributes to produce ultrafine grain size. The FSPed nano sized tensile specimen as shown in fig. 2.6 on the stir zone exhibited better mechanical properties than as received Al 5083 alloy. The wear properties of Al5083 alloy were improved by addition of B_4C nano particles in comparison with B_4C micro particle, and the wear resistance of the nano SCL was higher than that of unreinforced Al 5083 alloy.

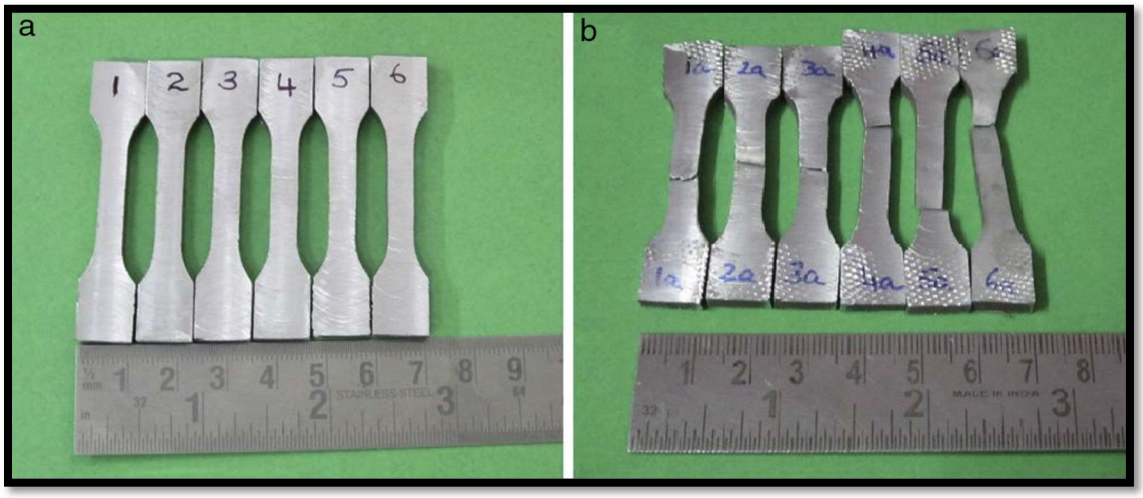

Fig.2.6: (a) Tensile specimens before tensile testing, (b) after testing. [16]

2.3.1 Tool Geometry

Tool geometry is the most influential aspect of composite fabrication as it affects the material flow and in turn governs the traverse rate at which FSP can be conducted. A FSP tool comprises of a shoulder and a pin.

In the initial stage of tool plunge, the heating results primarily from the friction between pin and work piece. The tool is plunged till the shoulder touches the work piece. The friction between the shoulder and work piece results in the biggest component of heating. From the heating aspect, the relative size of pin and shoulder is important.

I. Shoulder provides confinement for the heated volume of material.

II. The second function of the tool is to ‘stir' and 'move’ the material. The uniformity of microstructure and properties as well as process loads are governed by the tool design. Generally, a concave shoulder and threaded cylindrical pins are used. Whorl and Mx Triflute tools developed by TWI are pins for both tools are shaped as a frustum that displaces less material than a cylindrical tool of the same root diameter. Typically, the Whorl reduces the displaced volume by about 60%, while the MX Triflute reduces the displaced volume by about 70%. The design features of the Whorl and the MX Triflute are believed to
   a) Reduce processing force
   b) Enable easier flow of the plasticized material
   c) Increase the interface between the pin and the plasticized material

III. Increase the ratio between the swept volume and static volume of the pin, thereby improving the flow path around and underneath the pin

IV. Widen the processing region due to flared-out flute lands in the Flared-Trifute TM pin and the skew action in A-skew TM pin,

V. Provide an improved mixing action for oxide fragmentation and dispersal at the process interface, and

VI. Provide an orbital forging action at the root of the process due to the skew action, improving process quality in this region.

2.3.2 Tool Rotation, Transverse Speed, Tilt and Plunge

There are two tool speeds which are considered in a FSP – rotation speed and traverse speed. These two parameters have considerable importance and must be chosen with care to ensure a successful and efficient processing cycle. The relationship between the processing speeds and the heat input during processing is complex but, in general, it has been observed that increasing the rotation speed or decreasing the traverse speed result higher heat generation.

B. Zahmatkesh et al [19] observed hardness profile that on increased travelling speeds caused significant increment on the hardness values for all rotational speeds for the plain specimens and found the highest hardness value was 80 and the lowest was 37 for the plain

specimens however, increased rotation speeds resulted in lower hardness values at the same travelling speeds and observed in the bend test that the plain FSP treated surface was much more ductile and had lower yield strength as compared with SiC added specimen.

Plunging the shoulder below the plate surface increases the pressure below the tool and helps ensure adequate forging of material at the rear of the tool. Tilting the tool by 1-2 degrees, such that the rear of the tool is lower that the front, has been found to assist this forging process as shown in fig. 2.7. To ensure the necessary downward pressure is achieved and to ensure the total fully penetrates the process. Given the high loads required, the processing machine may deflect and so reduce the plunge depth compared to the nominal setting, which may result in flaws in the process.

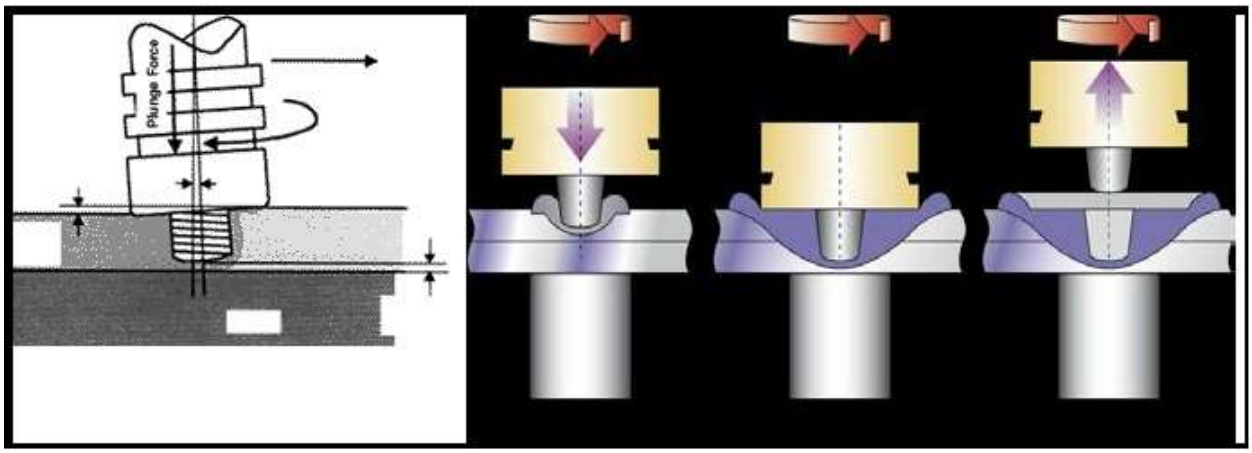

Fig. 2.7: Schematic of Tool Tilt and Tool Plunge [19]

2.3.3 Tool Material

Materials such as aluminum and magnesium alloys, and aluminum matrix composites (AMC) are commonly processed using steel tools. For FSP of AMCs, some studies have shown that the tool wears initially and obtains a self-optimized shape after which wear becomes much less pronounced. Tool wear was found to increase with rotational speed and decrease at lower transverse speed, which suggests that process parameters can be adjusted to increase tool life. M 35 Hot Work Tool Steel having a cylindrical pin of length 4 mm was used for processing.

2.3.4 Axial Load and Number of passes

Chandan et al [20] found that the triple pass FSP sample showed very fine uniformly distributed alloy silicide in a matrix of aluminum without any crack with respect to that of single pass, double pass, base metal which also coarse microstructure, and second pass have fine distributed silicides but not uniform. Single pass microstructure showed some surface defects with distribution of silicide shows discontinuity. So the mechanical properties are directly related with the fine microstructure. Kim Y. G. et al [21] found that material flow in the weld zone is influenced by the extrusion process, where the applied axial force and the motion of the tool pin propel the material after it has undergone the plastic deformation. The shoulder force is directly responsible for the plunge depth of the tool pin into the work-piece and load characteristics associated with linear friction stir welding**.** Kumar et al [22] studied on the role of axial load and the effect of interface position on the tensile strength of a friction stir welded aluminium alloy, and found **as** the axial load increases, both hydrostatic pressure beneath the shoulder and the temperature in the stir zone will increase. It is well known that the lower axial load results in defect in the weld because of insufficient coalescence of transferred material. Ouyang et al [23] reported that at steady state, the shoulder force varies depending upon the rotation speed. An increase in the rotation speed results in drop in the initial axial force with increasing time. The difference in the measured forces is due to decrease of the material flow stress at elevated weld temperature. Krishnan et al [24] studied the mechanism of onion ring formation in the friction stir welds of aluminum alloys and found that the degree of material mixing and inter-diffusion, the thickness of deformed aluminum lamellae and material flow patterns highly depend upon the geometry of the tool, welding temperature, and material flow stress in turn depends on the axial force. More no. of passes increases the distribution level of the particles properly. Hence, the mechanical properties and wear properties enhances.

2.4 Material Testing

2.4.1 Hardness Test

Hardness is the property of a material that enables it to resist plastic deformation, usually by penetration. It may also refer to resistance to bending, scratching, abrasion or cutting. An example would be material B scratches material C, but not material A. Alternatively, material A scratches material B slightly and scratches material C heavily. The usual method to achieve a hardness value is to measure the depth or area of an indentation left by an indenter of a specific shape, with a specific force applied for a specific time. There are three principal standard test methods for expressing the relationship between hardness and the size of the impression, these being Brinell, Vickers, and Rockwell.

For practical and calibration reasons, each of these methods is divided into a range of scales, defined by a combination of applied load and indenter geometry.

1. **Rockwell Hardness Test [25]**

   The Rockwell hardness test method as shown in fig. 2.8 consists of indenting the test material with a diamond cone or hardened steel ball indenter. The indenter is forced into the test material under a preliminary minor load F0 usually 10 kgf. When equilibrium has been reached, an indicating device, which follows the movements of the indenter and so responds to changes in depth of penetration of the indenter is set to a datum position. While the preliminary minor load is still applied an additional major load is applied with resulting increase in penetration. When equilibrium has again been reach, the additional major load is removed but the preliminary minor load is still maintained. Removal of the additional major load allows a partial recovery, so reducing the depth of penetration. The permanent increase in depth of penetration, resulting from the application and removal of the additional major load is used to calculate the Rockwell hardness number. Advantages of the Rockwell hardness method include the direct Rockwell hardness number readout and rapid testing time.

   Disadvantages include many arbitrary non-related scales and possible defects from the specimen support anvil.

   HR = E - e

F0 = preliminary minor load in kgf

F1 = additional major load in kgf

F = total load in kgf

e = permanent increase in depth of penetration due to major load F1 measured in units of 0.002 mm

E = a constant depending on form of indenter: 100 units for diamond indenter, 130 units for steel ball indenter

HR = Rockwell hardness number

D = diameter of steel ball

Rockwell Hardness Scales:

Table 2.1: Rockwell Hardness Scales [25]

Scale	Indenter	Minor Load *F0* kgf	Major Load *F1* kgf	Total Load *F* kgf	Value of *E*
A	Diamond cone	10	50	60	100
B	1/16" steel ball	10	90	100	130
C	Diamond cone	10	140	150	100
D	Diamond cone	10	90	100	100
E	1/8" steel ball	10	90	100	130
F	1/16" steel ball	10	50	60	130
G	1/16" steel ball	10	140	150	130
H	1/8" steel ball	10	50	60	130
K	1/8" steel ball	10	140	150	130
L	1/4" steel ball	10	50	60	130
M	1/4" steel ball	10	90	100	130
P	1/4" steel ball	10	140	150	130
R	1/2" steel ball	10	50	60	130
S	1/2" steel ball	10	90	100	130
V	1/2" steel ball	10	140	150	130

Application of Rockwell Hardness Scales:

HRA... Cemented carbides, thin steel and shallow case hardened steel

HRB... Copper alloys, soft steels, aluminium alloys, malleable irons,

HRC... Steel, hard cast irons, case hardened steel HRD... Thin steel and medium case hardened steel and pearlitic malleable iron

HRE... Cast iron, aluminium and magnesium alloys, bearing metals

HRF... Annealed copper alloys, thin soft sheet metals

HRG... Phosphor bronze, beryllium copper, malleable irons

HRH... Aluminium, zinc, lead

HRK/L/M/P/R/S/V...} Soft bearing metals, plastics and other very soft materials

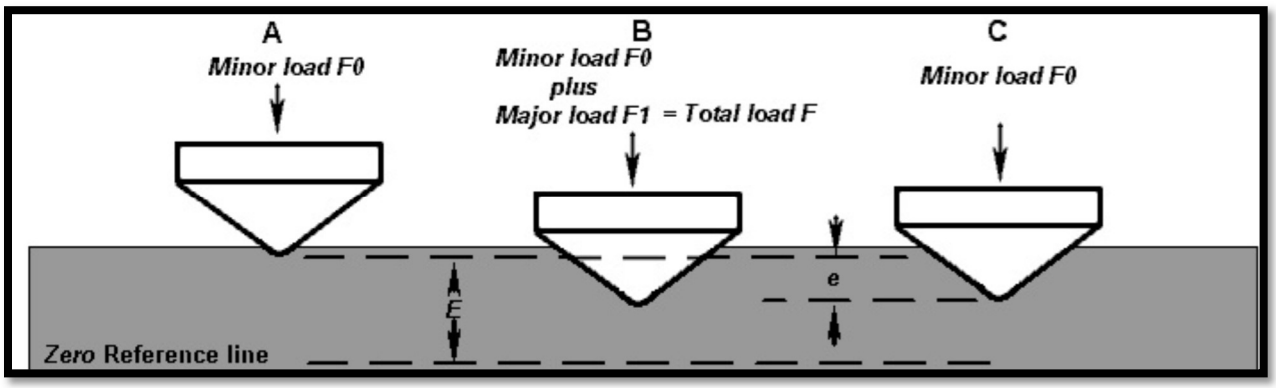

Fig. 2.8: Rockwell Hardness Principle [25]

2. **Brinell Hardness Test [26]**

The Brinell test, consists of applying a constant load or force, usually between 500 and 3000 Kgf, for a specified time (from 10 - 30 seconds) using a 5 or 10 mm diameter tungsten carbide ball. The load time period is required to ensure that plastic flow of the metal has ceased. Lower forces and smaller diameter balls are sometimes used in specific applications, only a single test force is applied. After removal of the load, the resultant recovered round impression is measured across diagonals at right angles and is usually recorded millimeters using a low-power microscope or an automatic measuring device.

The actual Brinell hardness (BHN) is calculated by factoring the indent size and the test force however it is not necessary to make the actual calculation for each test. Calculations have already been made and are available in tabular form for various combinations of diameters of impressions and load. In addition, various forms of automatic Brinell reading devices are available to perform these tasks.

It is typically used in testing aluminium and copper alloys (at lower forces) and steels and cast irons at the higher force ranges. Highly hardened steel or other materials are usually not tested by the Brinell method, also particularly useful in certain material finishes as it is more tolerant of surface conditions due to the indenter size and heavy applied force.

$$BHN=\frac{2P}{\pi D(D-\sqrt{(D^2-d^2)})}$$

where,

P=Force Applied

D=Diameter of Ball

d=Diameter of depression on sample

3. Vickers Hardness Test [27]

The Vickers hardness test method as shown in fig. 2.9 consists of indenting the test material with a diamond indenter, in the form of a right pyramid with a square base and an angle of 136 degrees between opposite faces subjected to a load of 1 to 100 kgf. The full load is normally applied for 10 to 15 seconds. The two diagonals of the indentation left in the surface of the material after removal of the load are measured using a microscope and their average calculated. The area of the sloping surface of the indentation is calculated. The Vickers hardness is the quotient obtained by dividing the kgf load by the square mm area of indentation.

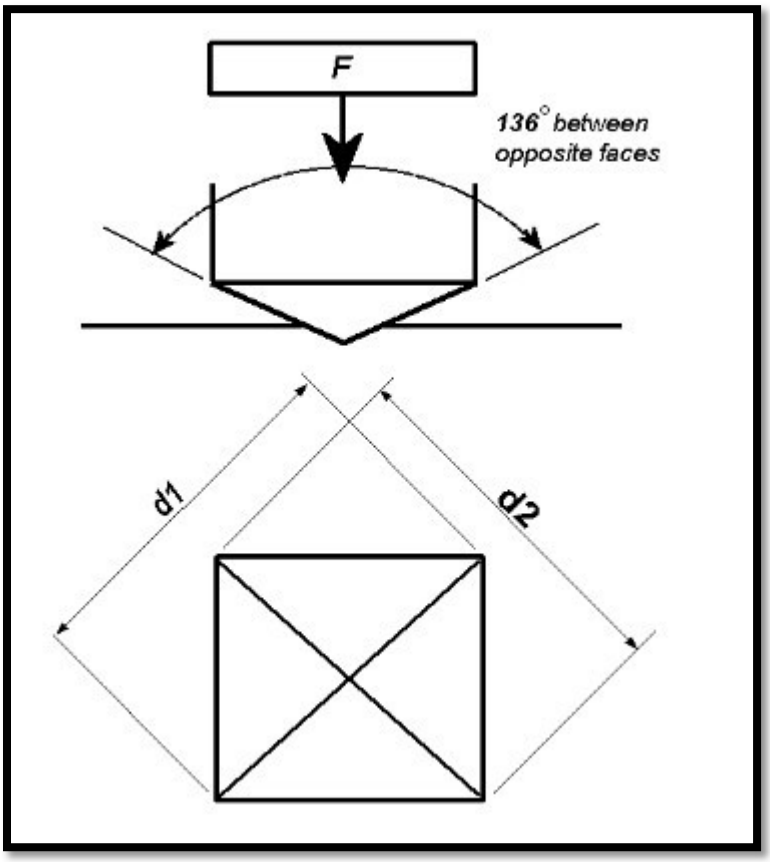

Fig. 2.9: Vicker Hardness Test [27]

F= Load in kgf

d = Arithmetic mean of the two diagonals, d1 and d2in mm

HV = Vickers hardness

$$HV = \frac{2F\sin\frac{136^{o}}{2}}{d^{2}} \qquad HV = 1.854\frac{F}{d^{2}} \text{ approximately}$$

When the mean diagonal of the indentation has been determined the Vickers hardness may be calculated from the formula, but is more convenient to use conversion tables. The Vickers hardness should be reported like 800 HV/10, which means a Vickers hardness of 800, was obtained using a 10 kgf force. Several different loading settings give practically identical hardness numbers on uniform material, which is much better than the arbitrary changing of scale with the other hardness testing methods. The advantages of the Vickers hardness test are that extremely accurate readings can be taken, and just one type of indenter is

used for all types of metals and surface treatments. Although thoroughly adaptable and very precise for testing the softest and hardest of materials, under varying loads, the Vickers machine is a floor standing unit that is more expensive than the Brinell or Rockwell machines. The conversion chart is shown in fig. 2.10

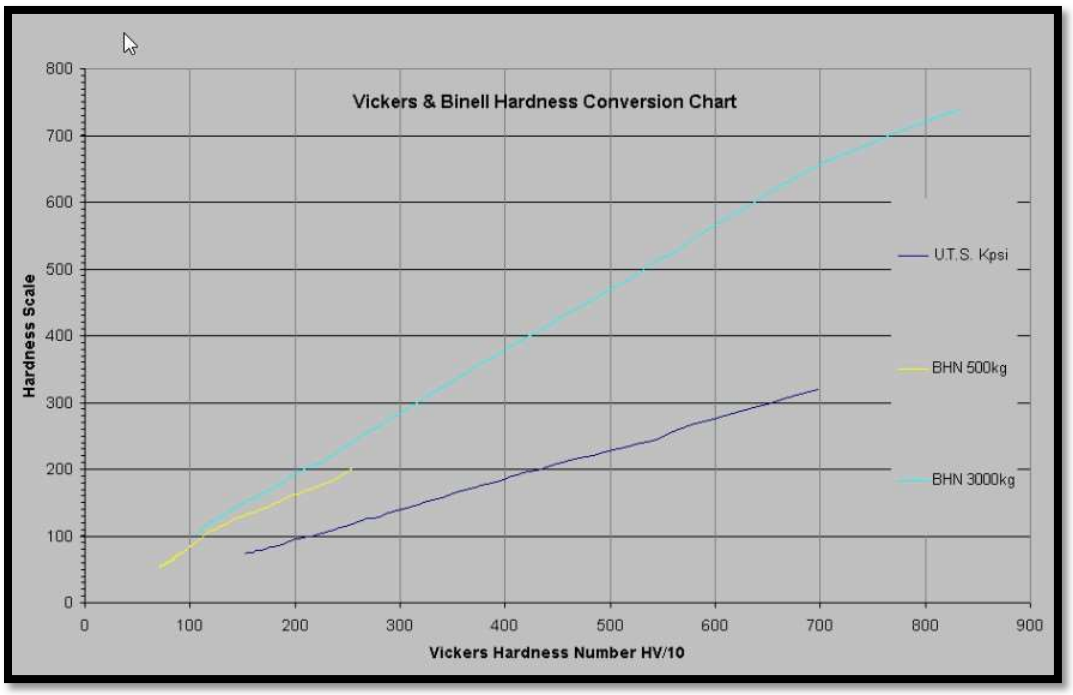

Fig. 2.10: Vickers and Brinell Conversion chart [27]

.

2.4.2 Tensile Test [28, 29]

Sample is subjected to a controlled tension until failure. The results from the test are commonly used to select a material for an application, for quality control, and to predict how a material will react under other types of forces. This test gives a measure of ultimate tensile strength, maximum elongation and reduction in area. From these measurements the following properties can also be determined: Young's modulus, Poisson's ratio, yield strength, and strain-hardening characteristics. Uniaxial tensile testing is the most commonly used for obtaining the mechanical characteristics of isotropic materials. For anisotropic materials, such as composite materials and textiles,

biaxial tensile testing is required. The plot we generate after tensile test between stress and strain is shown in fig. 2.11.

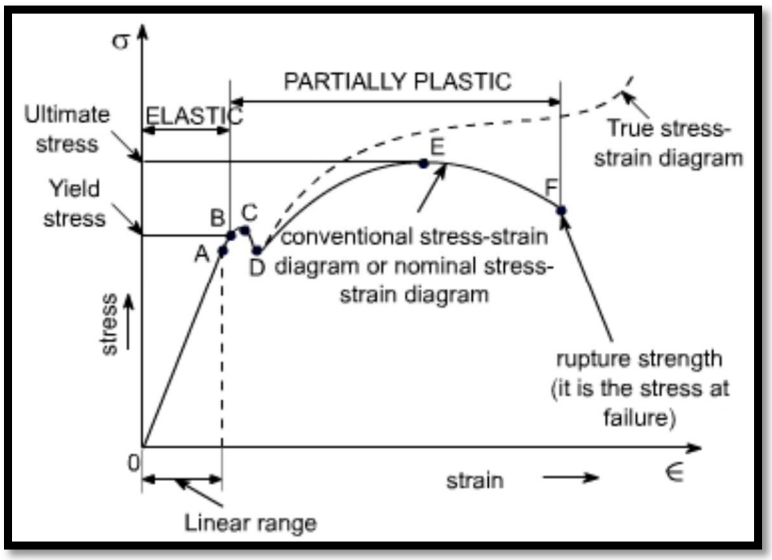

Fig. 2.11: Stress-Strain Curve [28]

Modulus of Elasticity:

The modulus of elasticity is a measure of the stiffness of the material. If a specimen is loaded within this linear region, the material will return to its exact same condition if the load is removed. At the point that the curve is no longer linear and deviates from the straight-line relationship, Hooke's Law no longer applies and some permanent deformation occurs in the specimen. This point is called the "elastic, or proportional limit". From this point on in the tensile test, the material reacts plastically to any further increase in load or stress. It will not return to its original, unstressed condition if the load were removed.

Tensile specimen as shown in fig. 2.12 is a standardized sample cross-section. It has two shoulders and a gauge (section) in between. The shoulders are large so they can be readily gripped, whereas the gauge section has a smaller cross-section so that the deformation and failure can occur in this area.

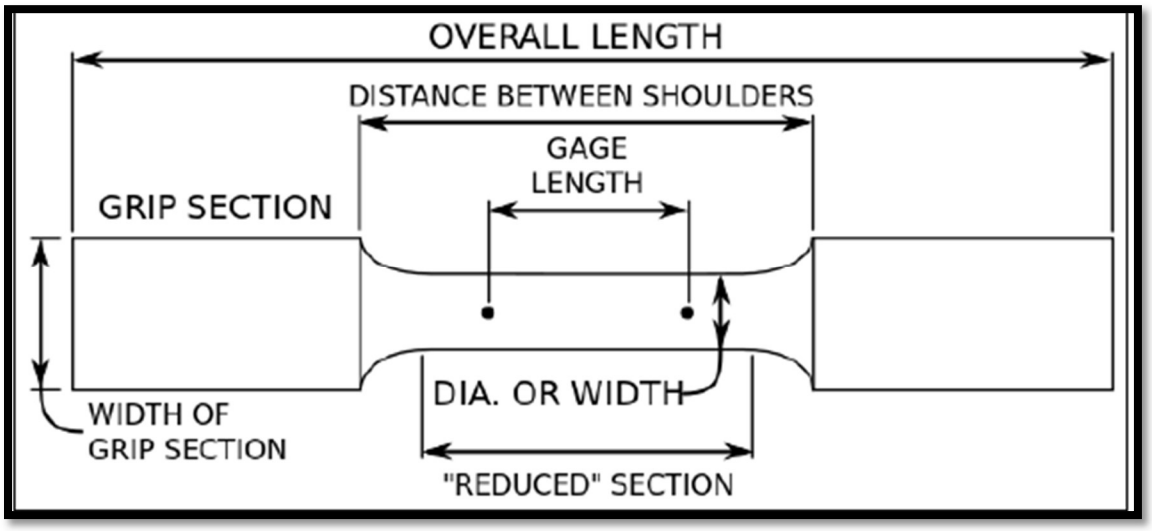

Fig. 2.12: Tensile Specimen Nomenclature [28]

Yield Strength:

A value called "yield strength" of a material is defined as the stress applied to the material at which plastic deformation starts to occur while the material is loaded.

Strain:

It is referred to as the amount of stretch or elongation the specimen undergoes during tensile testing, this can be expressed as an absolute measurement in the change in length or as a relative measurement called "strain".

Ultimate Tensile Strength:

This is the maximum load the specimen sustains during the test. The UTS may or may not equate to the strength at break. It depends on what type of material brittle, ductile or a substance that even exhibits both properties. And sometimes a material may be ductile when tested in a lab, but, when placed in service and exposed to extreme cold temperatures, it may transition to brittle behavior.

2.4.3 Microstructure Analysis

With optical microscopy, the light microscope is used to study the microstructure; optical illumination systems are its basic elements. For materials that are opaque to

visible light (all metals, many ceramics and polymers), only the surface is subject to observation, and the light microscope must be used in a reflective mode. Contrasts in the image produced result from differences in reflectivity of the various regions of the microstructure.

2.4.4 Scanning electron microscope [30, 31]

SEM testing as shown in fig. 2.13 is done for high resolution and magnification imaging with enhanced depth of field for trace evidence and non-destructive elemental analysis of gunshot residue particles, paint, metals, powders, and other trace particulate material. These components are part of seven primary operational systems: vacuum, beam generation, beam manipulation, beam interaction, detection, signal processing, and display and record. These systems function together to determine the results and qualities of a micrograph such as magnification, resolution, depth of field, contrast, and brightness.

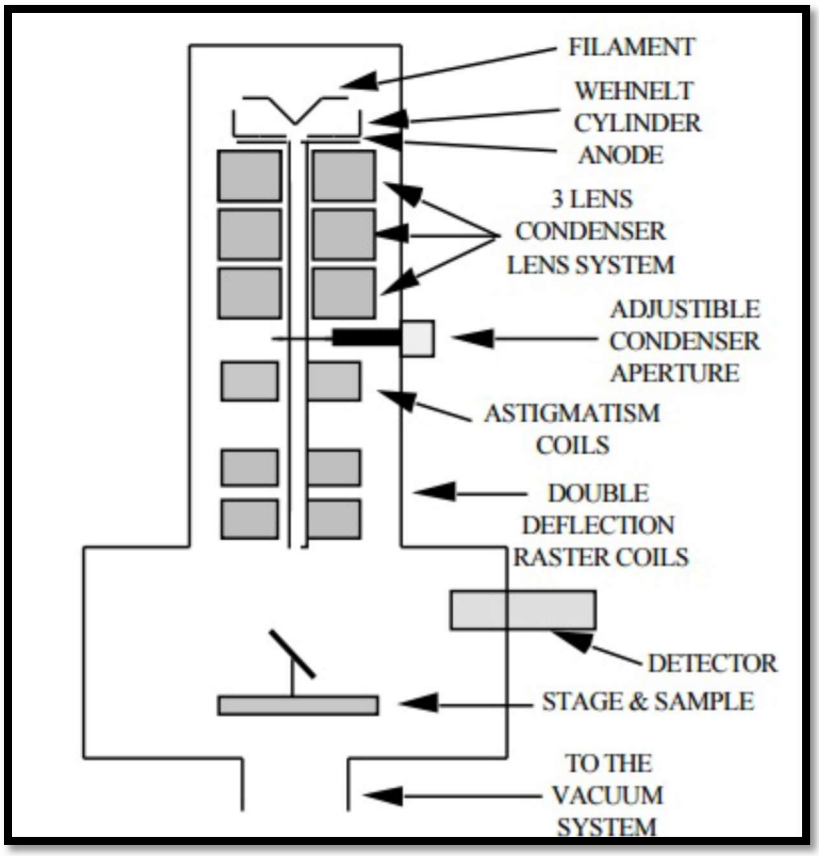

Fig. 2.13: Pictorial diagram of SEM with Column & Specimen

a) Vacuum system: A vacuum is required when using an electron beam because electrons will quickly disperse or scatter due to collisions with other molecules.
b) Electron beam generation system: This system is found at the top of the microscope column. This system generates the "illuminating" beam of electrons known as the primary (1o) electron beam.
c) Electron beam manipulation system: This system consists of electromagnetic lenses and coils located in the microscope column and control the size, shape, and position of the electron beam on the specimen surface.
d) Beam specimen interaction system: This system involves the interaction of the electron beam with the specimen and the types of signals that can be detected.
e) Detection system: This system can consist of several different detectors, each sensitive to different energy / particle emissions that occur on the sample.
f) Signal processing system: This system is an electronic system that processes the signal generated by the detection system and allows additional electronic manipulation of the image.
g) Display and recording system: This system allows visualization of an electronic signal using a cathode ray tube and permits recording of the results using photographic or magnetic media.

2.4.5 Wear Test

Wear Test is done to evaluate the weight loss, wear rate and coefficient of friction (COF) between pin and disc. There are various process and machines available for this purpose. We used pin on disc tribometer. Pin on disc Wear Testing is a method of characterizing COF, frictional force and rate of wear between two materials. During the tribological test, a stationary disk articulates against a rotating pin while under a constant applied load.

2.5 Research Gap

On the basis of literature survey it has been observed that mechanical and tribological properties enhances as well as hardness of the work-piece increase after FSP. Observation with boron carbide and silicon carbide reinforced particles using FSP on AA6061-T6 has not been done till now. So, it is necessary to observe the behavior using boron and silicon carbide as a reinforcement with FSP.

2.6 Objectives

The present work aims at studying the FSP of AA 6061. On the basis of literature survey, the following research objectives have been drawn.

a) To design and fabricate the tool used for Friction Stir Processing.
b) To conduct the experimental study with boron carbide, silicon carbide and mixture of both and without using any particles at a particular combination of process parameters.
c) To study the mechanical properties of friction stir processed (FSPed) work-piece.
d) To study the tribological behavior of friction stir processed (FSPed) work-piece.
e) To study the microstructure of friction stir processed (FSPed) work-piece with opticak microscope (OM) and scanning electron microscope (SEM).

2.7 Report Layout

The present thesis is organized into five chapters. The first chapter deals with a brief introduction to the work. The second chapter deals with a detailed literature review on the concept of FSP and on the basis of literature survey research objective are drawn. Third chapter explains the experimental methodology used for achieving the set objectives. Fourth chapter carries experimental work. Fifth chapter shows results and discussion. In the last chapter conclusion and future scope has been mentioned.

Chapter 3 EXPERIMENTAL PROCEDURE

In the present work, we intend to experimentally investigate the effects with and without various reinforced particles on the mechanical and tribological properties of the composite AA6061-T6.

3.1 Process Parameters

On the basis of literature review, following process parameters have been used during the experimental study as shown in table 3.1.

Table 3.1: Process parameters used in Friction Stir Processing

Process Parameters	Value
Transverse Speed of the Tool	25 mm/min
Axial load on Plate	8-9 KN
Rotational Speed of the Tool	1000 Rpm
No of Passes of Tool	3
Tool tilt angle	0 degree
Slot Design	1 mm (width)* 3 mm (depth)

3.2 Friction Stir Welding Machine Set up

An indigenous developed friction stir welding machine (R V machine tools, FSW-4T-HYD, shown in fig. 4.1) is used for Friction Stir Processing. Specifications of the machine are as follows:

- Power – 15 hp
- Rpm – 3000
- Load capacity – 25 KN
- Clamps – hydraulic actuated. Toe clamps are used to hold the job firmly
- Colet used for holding the tool could hold a cylindrical (tapered/un-tapered) tool of diameter 20mm.
- Backing plate groove – 200 mm × 80 mm

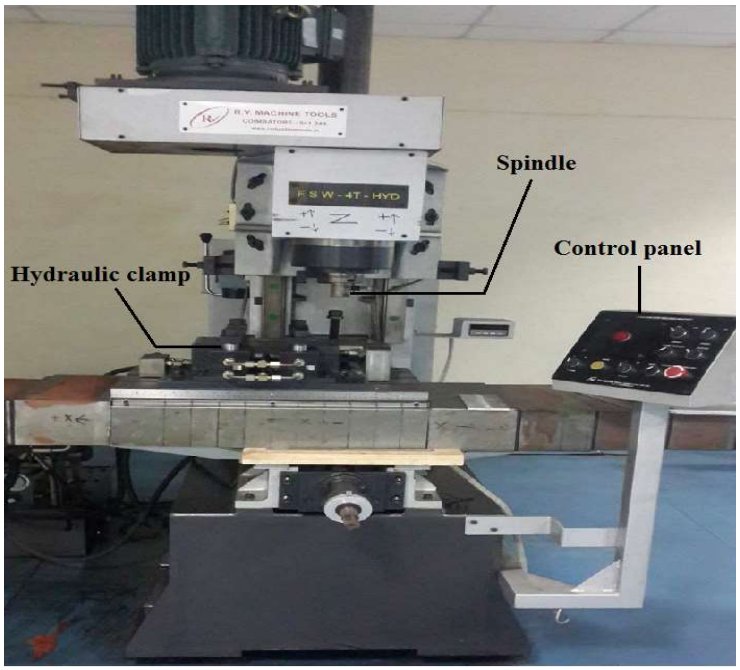

Fig. 3.1: Friction Stir Welding Machine

3.3 FSP Tool Specifications

Tool used during FSP (shown in fig.3.2) has following specifications:

- Tool Material: M35 Tool steel with max 5% cobalt for high hot hardness.
- Shoulder diameter of 24 mm.
- Pin size of 6 mm.
- Pin profile of cylindrical with threads of M6X1.
- Pin length of 4 mm.

Manufactured tool, draft, mass properties, chemical and physical composition is shown in fig. 3.2, fig. 3.3, fig. 3.4, fig. 3.5 and fig. 3.6 respectively.

Fig. 3.2: A Manufactured FSP tool

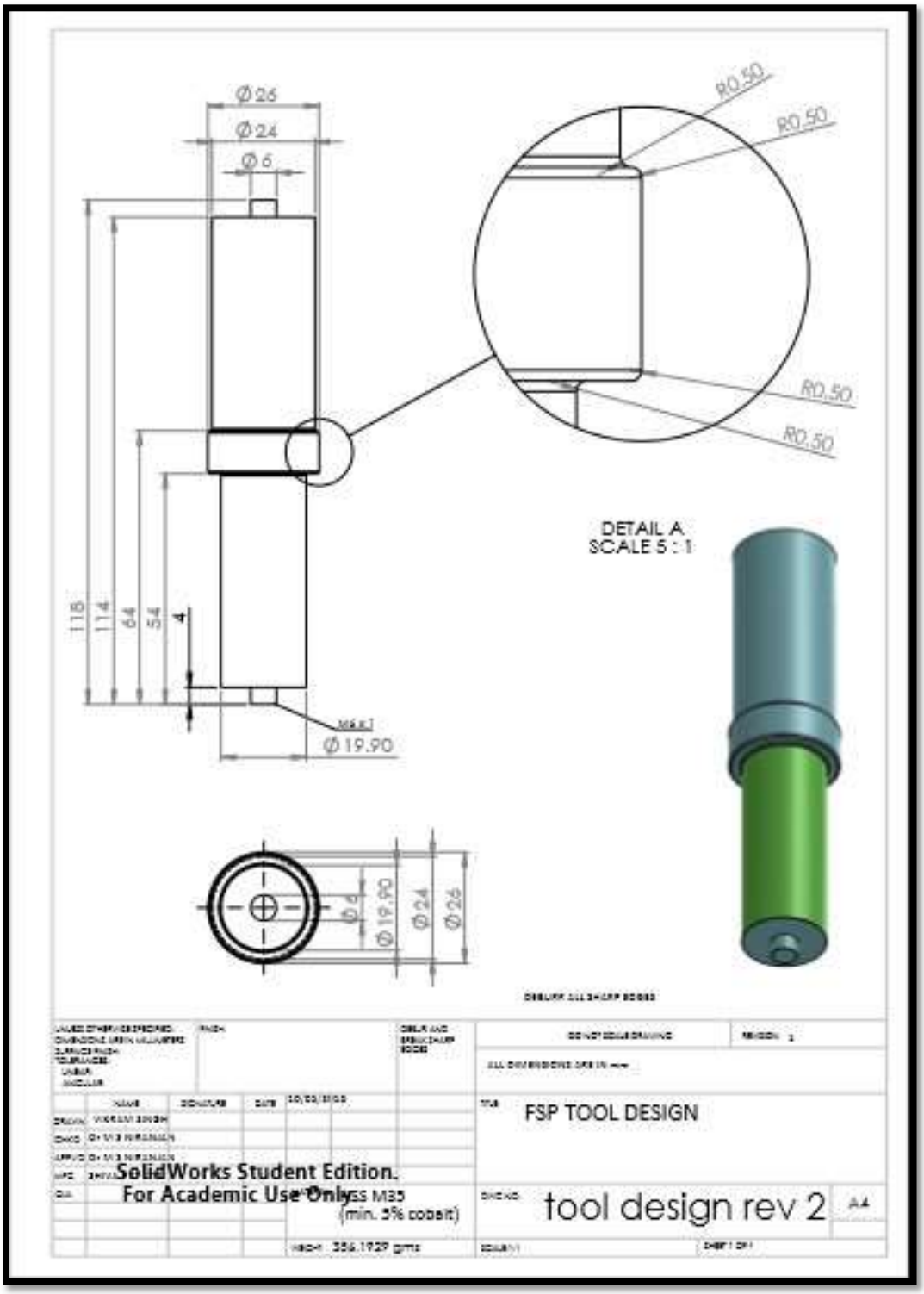

Fig. 3.3: Draft of Designed Tool using Solid works

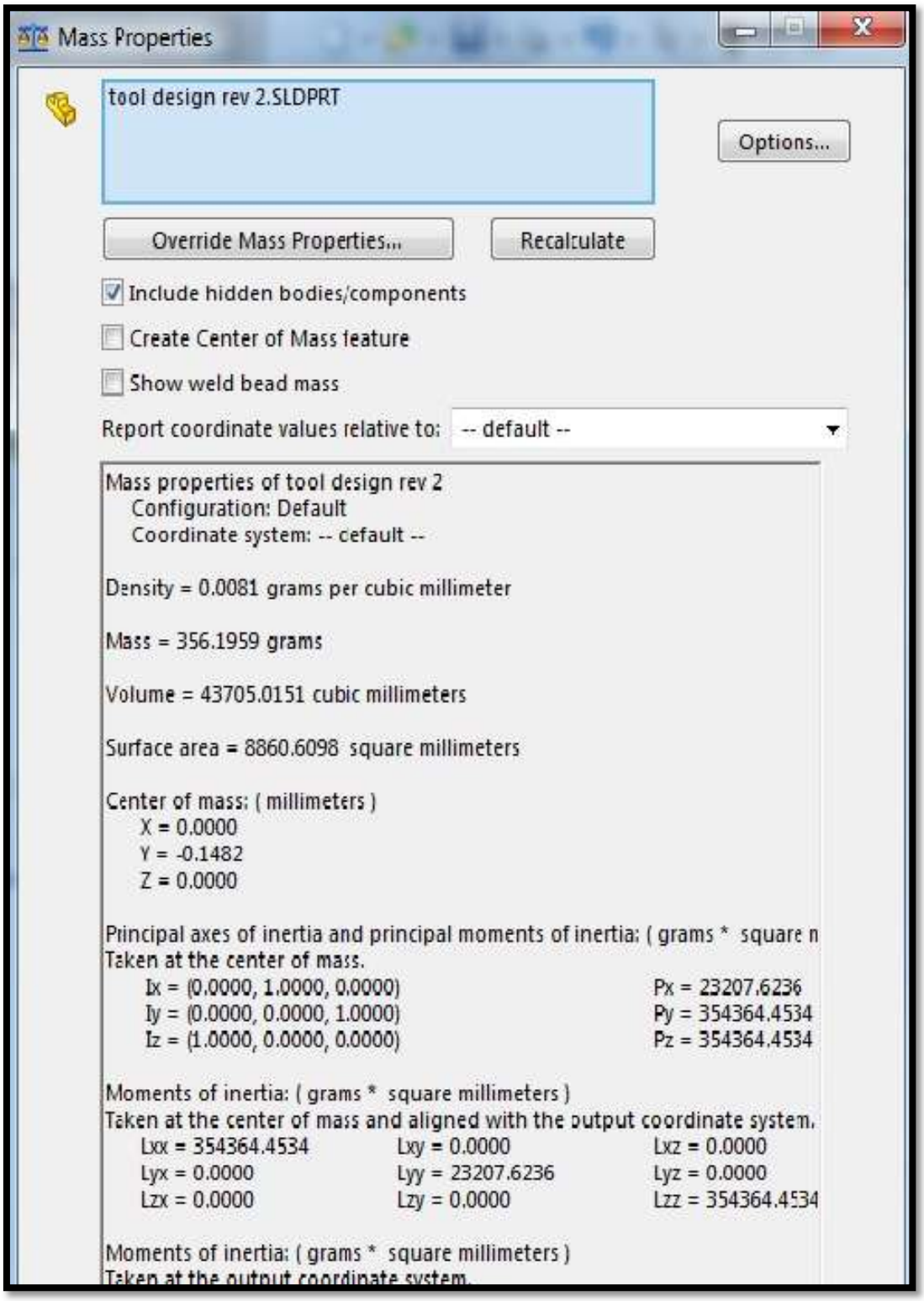

Fig. 3.4: Mass Properties of the Tool Using Solid Works

AISI HSS Tool Steel M35 material Chemical Composition Compparison

ASTM A600	C		Mn		P	S	Si		Cr		V		W		Mo		Co	
M35	0.82	0.95	0.15	0.40	0.03	0.03	0.20	0.45	3.80	4.50	1.75	2.15	5.5	6.75	4.75	5.25	4.60	5.00
DIN ISO 4957	C		Mn		P	S	Si		Cr		V		Mo		W		Co	
1.3243/HS6-5-2-5	0.87	0.95	...	...	...	...	...	0.45	3.80	4.50	1.70	2.10	4.70	5.20	5.90	6.70	4.50	5.00
JIS G4403	C		Mn		P	S	Si		Cr		V		Mo		W		Co	
SKH55	0.87	0.95	...	0.40	0.03	0.03	...	0.45	3.80	4.50	1.70	2.10	4.70	5.20	5.90	6.70	4.50	5.00

Fig. 3.5: Tool Composition [32]

- **M35 HSS Physical Properties**

		TEMPERATURE °C / °F		
		20 / 70	400 / 750	600 / 1110
Density	Kg/m³ lbs/in³	8150 .294	8050 .290	7990 .228
Modulus of Elasticity	kN/mm³² psi	230 34 · 10 6	205 31 · 10 6	184 27 · 10 6
Coefficient of Thermanl expansion from 20°C / 70°F	per °C per °F	–	11.6 · 10-6 6.4 · 10-6	11.9 · 10-6 6.6 · 10-6
Thermal Conductivity	W/m °C Btu/sq. ft. h °F/in.	24 166	28 194	27 187
Specific Heat	J/kg °C Btu/lb °F	420 0.10	510 0.12	600 0.14

Fig. 3.6: Tool Physical Properties [32]

3.4 Experimental Procedure

3.4.1 Al 6061 T6 Plate

AA6061 is a medium to high strength heat-treatable alloy with strength higher than 6005A. It has very good corrosion resistance and very good weldability although reduced strength in the weld zone. It has medium fatigue strength. It has good cold formability in the temper T4, but limited formability in T6 temper. Not suitable for very complex cross sections. The size of plates is (195 X 75 X 6) mm as shown in fig. 3.7.

Fig. 3.7: Slotted Plate before FSP

We have two plates with two slot each. Each plate is being leveled from the sides by using vertical milling machine shown in fig. 3.8. We processed it with different particles i.e. boron carbide, silicon carbide, with mixture of both and without any particles. The Plate is being designed in Solid works and drafted for vendor purpose. The drafted picture and mass properties is shown in fig. 3.9 and fig. 3.10.

Fig. 3.8: Leveling of plate in vertical milling machine

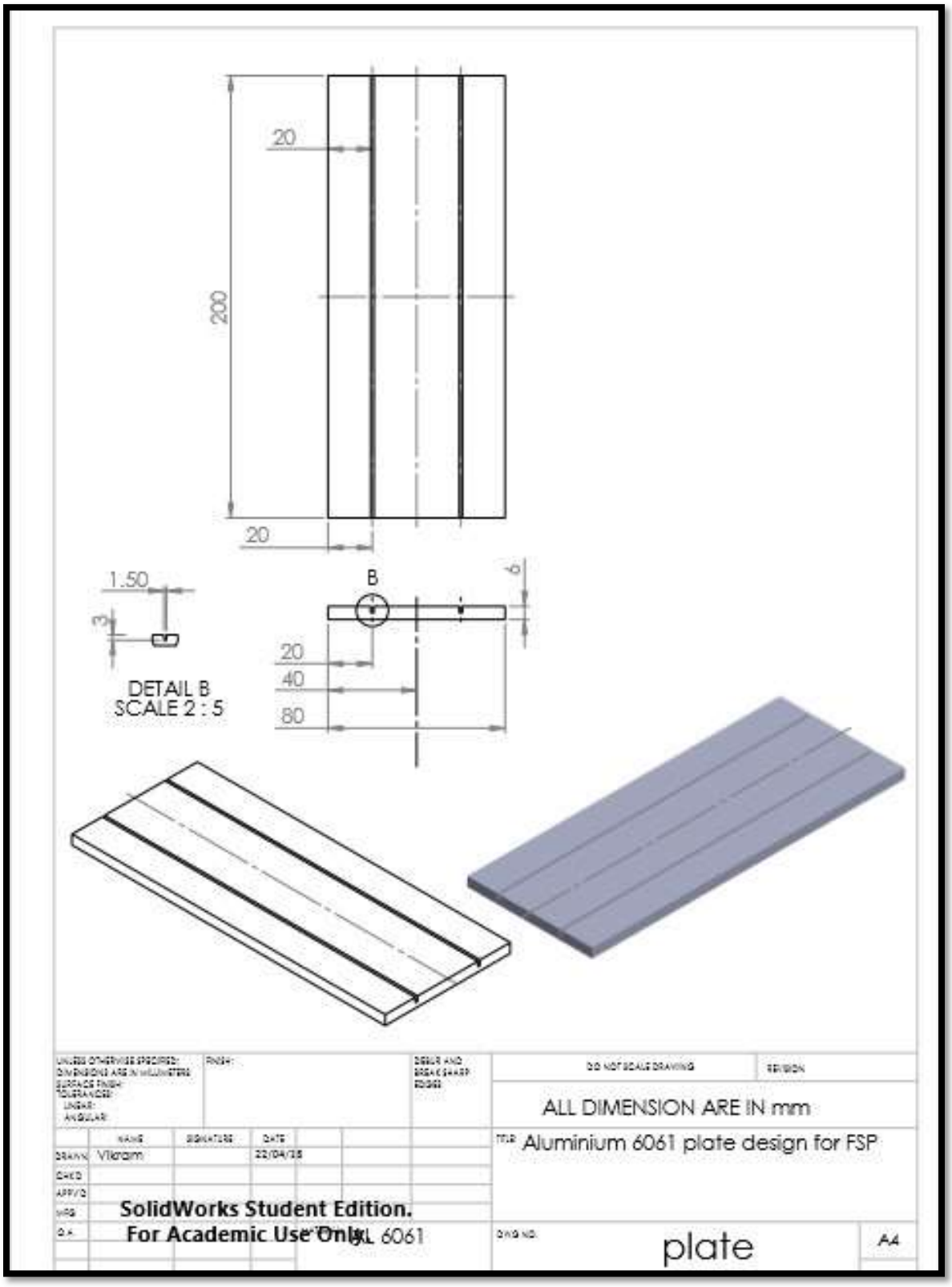

Fig. 3.9: Draft of Designed Plates

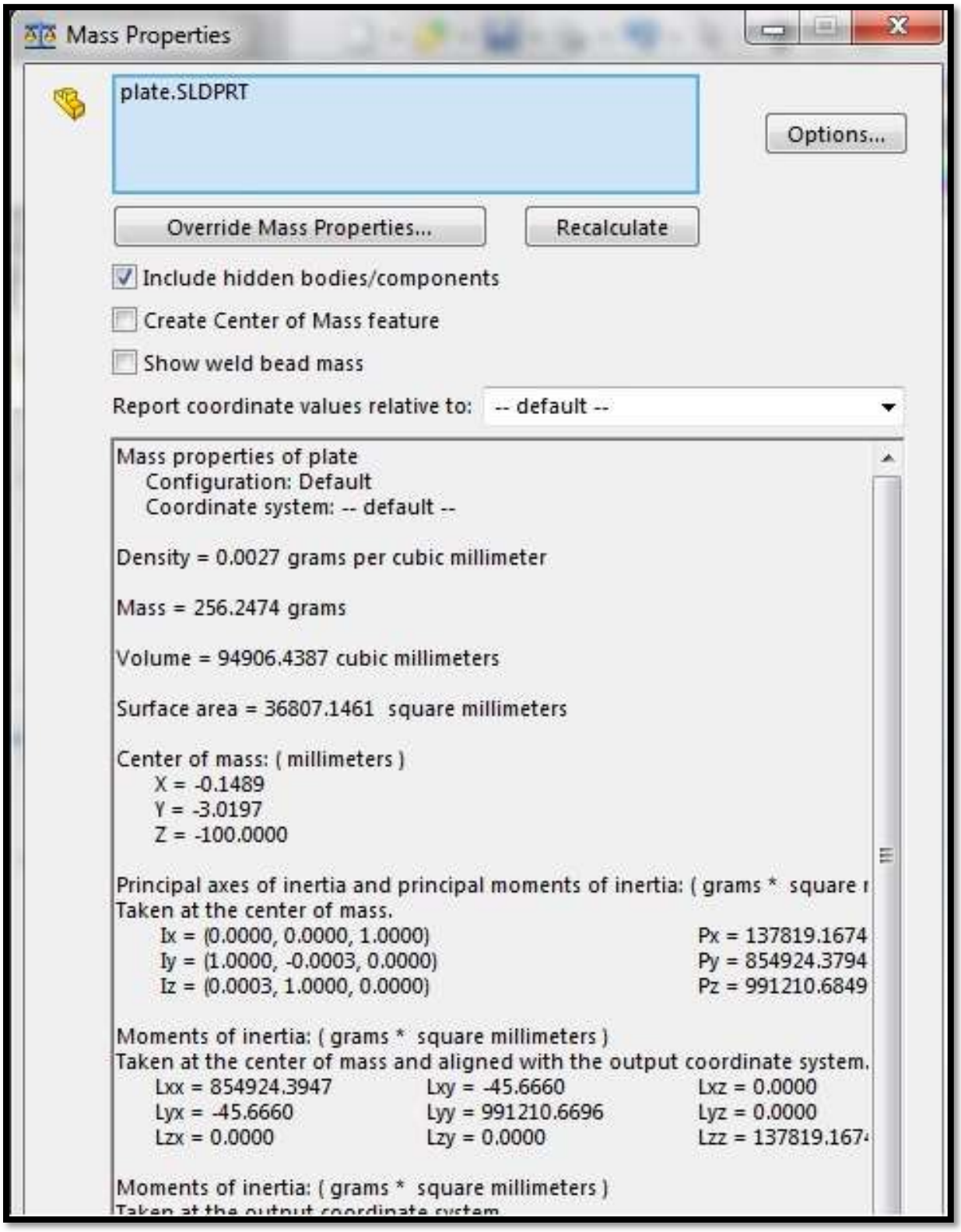

Fig 3.10: Mass Properties of plate by solid works

Chemical Composition:

Chemical composition of work-piece (plate) is shown in table 3.2

Table 3.2: Chemical Composition of Al 6061 T6 [34]

Element	Content (%)
Manganese, Mn	0.0-0.15
Iron, Fe	0.0-0.70
Magnesium, Mg	0.8-1.2
Silicon, Si	0.4-0.8
Copper, Cu	0.15-0.40
Zinc, Zn	0.0-0.25
Titanium, Ti	0.0-0.15
Chromium, Cr	0.04-0.35
Aluminium, Al	Balance

Physical Properties:

Physical Properties of work-piece (plate) is shown in table 3.3

Table 3.3: Physical Properties of Al 6061 T6 [34]

Physical Properties	**Value**
Density	2.70 g/cm3
Melting Point	650℃
Thermal Expansion	23.4 X 10^{-6}/K
Thermal Conductivity	166 W/mK
Electrical Resistivity	0.04 X10^{-6} Ω.m
Proof Stress	240 Typical MPa
Tensile Strength	260 Typical MPa
Hardness Brinell	86 Typical HB

3.4.2 Composite Fabrication

On a AA6061-T6 plate, the groove has been made after designing its dimensions. The slots or grooves have been filled with boron carbide & silicon carbide particles and mixture of both (1:1 ratio by vol.) respectively. Then the plate has been mounted on the bed of FSP machine rigidly with the help of clamps. Then the tool pin gets inside the slot in the plate and axial load is given to plate via tool shoulder. Tool will move forward doing extrusion and forging together. We will repeat this as per the no. of passes decided. Schematic view of the process is shown in fig. 3.11.

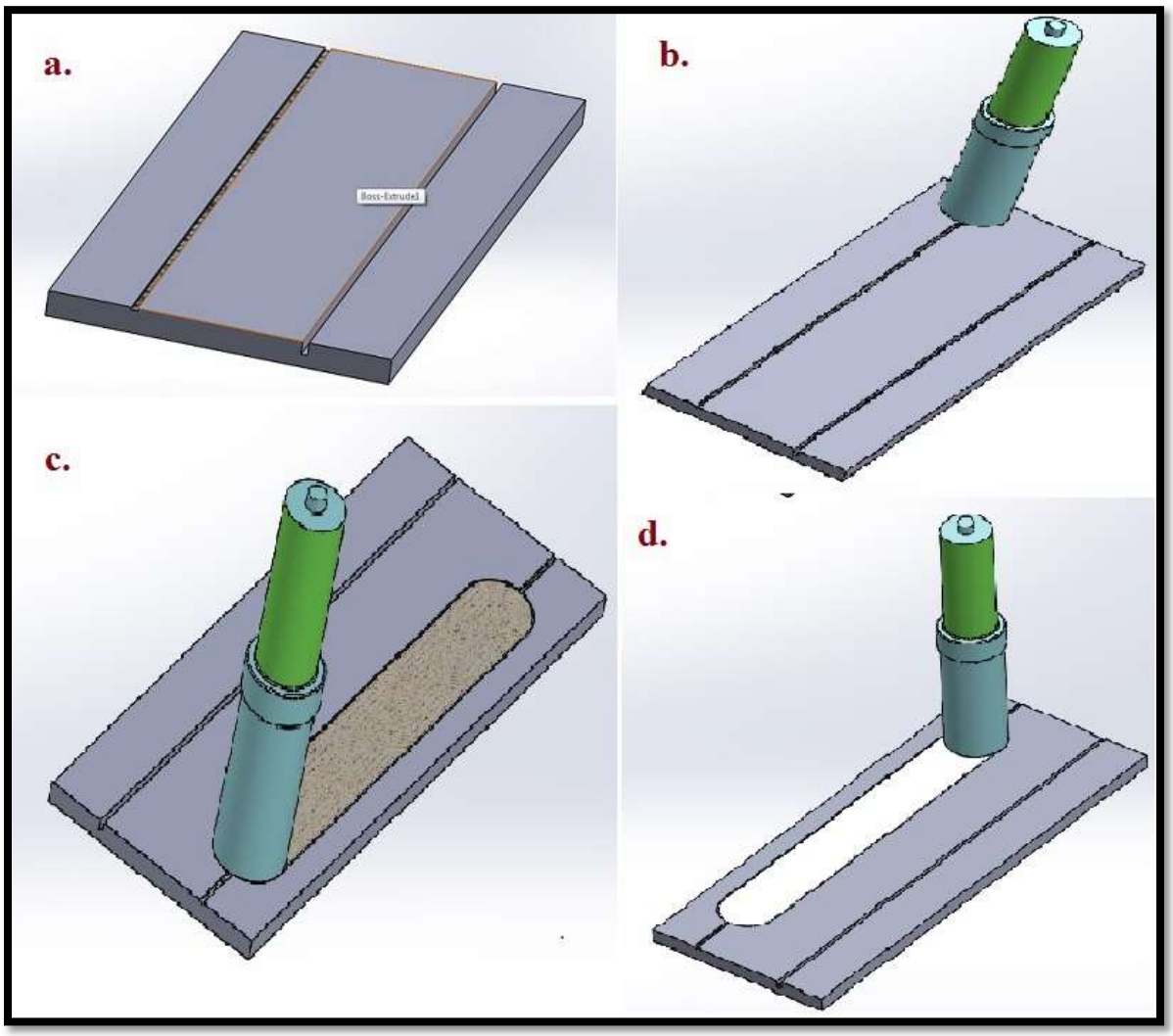

Fig. 3.11**:** (a) Plate with the slot filled with particles. (b) Plate with the tool for closing the slot. (c) Slot closed with the help of pin less tool. (d) Plate after Processing with the tool.

3.4.3 REINFORCEMENT: Boron Carbide (B_4C) and Silicon carbide (SiC)

Boron Carbide: (Mesh Size: 1000) [34]

Boron Carbide is one of the harder materials known, ranking third behind diamond and cubic boron nitride. It is the harder material produced in tonnage quantities. Originally discovered in mid-19th century as a by-product in the production of metal borides, boron carbide was only studied in detail since 1930. Boron carbide is mainly produced by reacting carbon with B_2O_3 in an electric arc furnace, through carbothermal reduction or by gas phase reactions. For commercial use B_4C powders usually need to be milled and purified to remove metallic impurities. In common with other non-oxide materials, boron carbide is difficult to sinter to full density, with hot pressing or sinter HIP being required to achieve greater than 95% of theoretical density. Even using these techniques, in order to achieve sintering at realistic temperatures (e.g. 1900 - 2200°C), small quantities of dopants such as fine carbon, or silicon carbide is usually required. Mechanical properties of boron and silicon carbide is given in table 3.4.

Table 3.4: Mechanical properties of boron carbide (B_4C) and Silicon Carbide (SiC) [34]

Property	Boron Carbide	Silicon Carbide
Density ($g.cm^{-3}$)	2.52	3.1
Melting Point (°C)	2445	2730
Hardness (Knoop 100g) ($kg.mm^{-2}$)	2900-3580	2800
Fracture Toughness ($MPa.m^{-½}$)	2.9 - 3.7	4.6
Young's Modulus (GPa)	450 - 470	410
Electrical Conductivity (at 25°C) (S)	140	170
Thermal Conductivity (at 25°C) (W/m.K)	30 - 42	120
Thermal Expansion Co-eff. $x10^{-6}$ (°C)	5	4

Silicon Carbide: (Mesh Size: 1000) [34]

Silicon carbide is a hard covalently bonded material predominantly produced by the carbothermal reduction of silica (typically using the Acheson process). Depending on the exact reaction conditions the resulting silicon carbide is either a fine powder or a bonded mass that requires crushing and milling to produce a usable feedstock. Several hundred structures of silicon carbide (polytopes) have been identified which have different stacking arrangements for the silicon and carbon atoms. The simplest structure is a diamond structure which is designated β-SiC. Other structures are either hexagonal or rhombic and are referred to as α-SiC. The outline properties of Silicon Carbide are that it is a refractory material (high melting point), it has excellent thermal conductivity and low thermal expansion, and consequently it displays good thermal shock resistance. In addition, the high hardness, corrosion resistance and stiffness lead to a wide range of applications where wear and corrosion resistance are primary performance requirements. Silicon carbide possesses interesting electrical properties due to its semiconductor characteristics, the resistance of different compositions varying by as much as seven orders of magnitude.

3.4.4 Hardness Test

a. Rockwell Hardness Test

Apparatus: Rockwell Hardness Test Machine, 4 FSPed samples

Procedure:

a) The indenter is “set” into the sample at a prescribed minor load. A major load is then applied and held for a set time period.
b) The force on the indenter is then decreased back to the minor load. The Rockwell hardness number is calculated from the depth of permanent deformation of the indenter into the sample, i.e. the difference in indenter position before and after application of the major load.
c) The minor and major loads can be applied using dead weights or springs. The indenter position is measured using an analog dial indicator.

d) The Rockwell hardness number is expressed as a combination of the measured numerical hardness value and the scale letter preceded by the letters, HR.

The Rockwell hardness test machine is shown in fig. 3.12

Fig. 3.12: Rockwell harness test machine, Rockwell no. indicator, Brinell hardness test machine (Left to right)

b. Brinell Hardness Test

Apparatus: Brinell Hardness Test Machine, 6 FSPed samples, stop watch

Procedure:

a) Procure all the samples for which testing is to be done. Switch on the Brinell Testing Machine.
b) Ensure the load P=750kgf, note down the reading for D (Diameter of Ball).
c) Place the sample with on the working bench, using sliding arrangement move the ball carrying mount and ensure it's tight on the sample.
d) Using load handle mount the load for a period of 10 seconds so that depression can be obtained.
e) Demount the load, without shifting the sample, using side sliding arrangement use the cross scales using screw gauge to obtain the diameter of depression.
f) Repeat steps c) to e) for other samples.

g) Record the observations and perform the necessary calculations to obtain the corresponding BHN value.

3.4.5 Tensile Test

Apparatus: Tensile Test Machine, 5 FSPed samples

Procedure:

a) Procure all the necessary samples, ensure proper markings are done using a permanent marker and the corresponding values of gauge length have been noted using digital Vernier calliper. Switch on the Tensile Testing Machine.

b) Mount the sample in the clamps. Input the required values for width, thickness and gauge length.

c) Start the test, wait patiently, save the test results comprising of Force-Displacement and Stress-Strain curves. De-clamp the sample.

d) Repeat steps b) & c) for other samples and record the relevant observations comprising of final gauge length and ultimate tensile strength.

Universal testing machine is shown in fig. 3.13

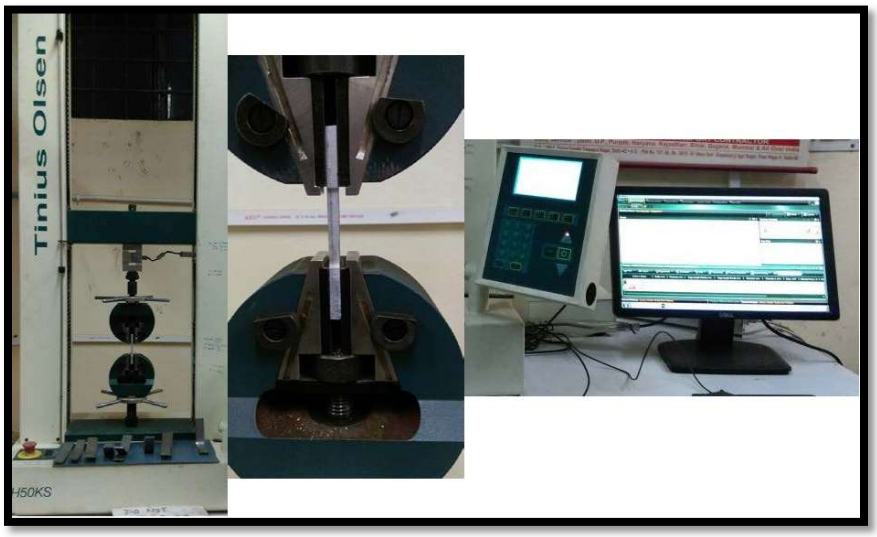

Fig. 3.13: Tensile Test Machine, Mounting, Control/ DAQ System (Left to Right)

3.4.6 Wear Test

Apparatus: TR 20 LE, 5 FSPed samples

Procedure:

a) The sliding test carried out using pin-on-disc machine (model TR 20 LE, manufactured by DUCOM, Bangalore, India).
b) Insert the specimen pin inside hardened jaw and clamp to specimen holder, set the specimen height above the wear plate and tighten the clamping screws on jaws to clamp specimen pin firmly.
c) Set required wear track radius by moving the sliding plate over graduated scale on the base plate and tighten all six no of clamping screws.
d) Pin of 10 mm diameter wear made to slide against EN-24 material disc of hardness 55 HRC and diameter 160 mm.
e) The track diameter kept constant at 100mm, disc speed was maintained at 382 rpm resulting in sliding velocity of 2 m/s and constant load 40N applied on each samples.
f) The wear track diameter and disc speed were kept constant during the entire experiment. Frictional force in kg and cumulative wear loss in mm measured from sensor output as a function of time.
g) The wear rates of the pins, defined as the cumulative wear suffered by the pin per unit sliding distance per unit load, were calculated from the cumulative data.
h) The worn samples surfaces were cleaned by acetone and examined under the scanning electron microscope.

The specifications of the machine are as follows:

- Wear track diameter: min 50 mm to max 100 mm
- Pin diameter: 4, 6, 8, 10, 12 mm
- Disc size: 165 mm diameter and 8 mm thickness
- Disc material: EN-24 hardened to 55 HRC
- Disc rotation speed: 200 to 2000 rpm continuously variable with digital tachometer

- Frictional force: 0 to 200N digital read out with recorder output
- Sliding speed: min 0.5m/s to max 10 m/s
- Normal load: 1N to 200N
- Wear range: -2mm to 2mm

Pin on disc tribometer is shown in fig. 3.14

Fig. 3.14**:** Pin on disc Tribometer experimental setup

3.5 Repeatability

Repeatability or test–retest reliability is the variation in measurements taken by a single person or instrument on the same item, under the same conditions, and in a short period of time. A less-than-perfect test–retest reliability causes test–retest variability. Such variability can be caused by, for example, intra-individual variability and intra-observer variability. A measurement may be said to be repeatable when this variation is smaller than a pre-determined acceptance criterion. In the case of composite fabrication, the following parameters will hold a lot of importance-

i. Base Alloy Plates: Different manufacturers use different sequences and procedures which vary with time even if purchased from the same manufacturer.
ii. Grooving Operation: The dimensions of groove, surface finish depends on the type of machine used for grooving. This will further depend on how many times the blade has been used, the machine has been serviced and calibrated.
iii. Reinforcement Paste Preparation: The exact densities of ceramic reinforcements can never be determined so in reality an actual correct ratio cannot be repeated these variations will affect the repeatability of fabrication.
iv. Filling of slots: The amount of reinforcement that can be filled in a given slot depends on the observer, the amount of hand force, the type of reagent used and the application mechanism used.
v. Vertical Milling Machine Parameters: These include tool rotation speed, traverse speed, downforce & tilt angle.
vi. Regular Calibration and Maintenance: The equipment and tools should be regularly calibrated and properly serviced. But still due to dynamic variations, deviations are bound to exist.
vii. Test equipment: The test procedures and apparatus utilised to analyse a test specimen also affects repeatability

The primary aim is to minimize these deviations by ensuring utilization of same experimental tools, same observer, measuring instrument, under same conditions, location, repetition over a short period of time and same objectives.

Chapter 4 EXPERIMENTAL WORK

4.1 Material Fabrication

The composite fabrication of Al6061T6 with Silicon Carbide and Boron Carbide and both of them as a reinforcement particles have been successfully completed on 4 samples with 3 passes in FSP as shown in fig. 4.1. These 4 samples are listed below-

I. Sample 1: Al6061T6 with 12.5 vol. % Silicon Carbide.

II. Sample 2: Al6061T6 with 12.5 vol.% Boron Carbide .

III. Sample 3: Al6061T6 with 6.25 vol.% each Boron carbide and silicon carbide (mixture) both.

IV. Sample 4: Al 6061T6 without reinforced particles.

Fig. 4.1: Processed Plate.

The volume fraction of B_4C and SiC are calculated using the following expression:

Volume fraction = (Area of groove/Projected area of Tool Pin) * 100

4.2 Specimen Formulation

The necessary specimens were prepared from the processed samples and obtained from the center of the Surface Composite Layer (SCL) using EDM Wire cut machine.

- The longitudinal tensile specimen prepared on the middle FSP stir zone by wire EDM as per E8/E8M-011 standard as shown in fig. 4.2.
- Wear test specimen of 10 mm diameter are cut from the middle of the stirred zone of FSPed surface by wire EDM. Wear test are conducted as per the ASTM G99-04 standard. Wear specimen with attached to pin for test is shown in fig. 4.5.
- Hardness and microstructure test specimen of 10mm x 10mm x 6mm wire cut from FSPed stir zone.
- All the wire cut specimen from the SCL are shown below in the fig. 4.4.

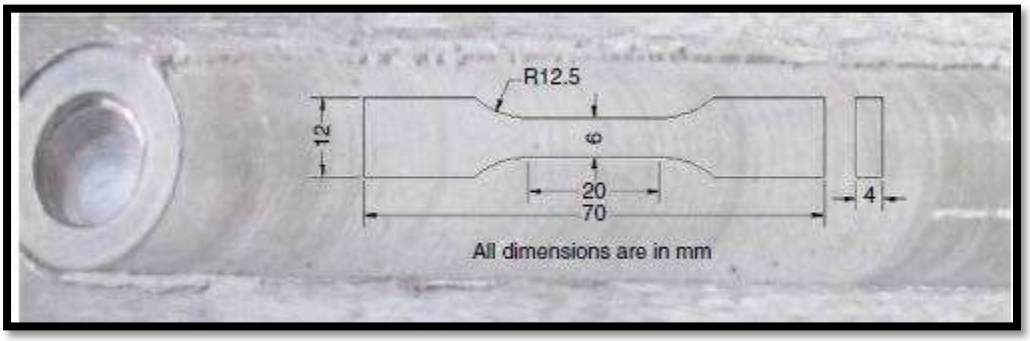

Fig. 4.2: Tensile Specimen Dimensions.

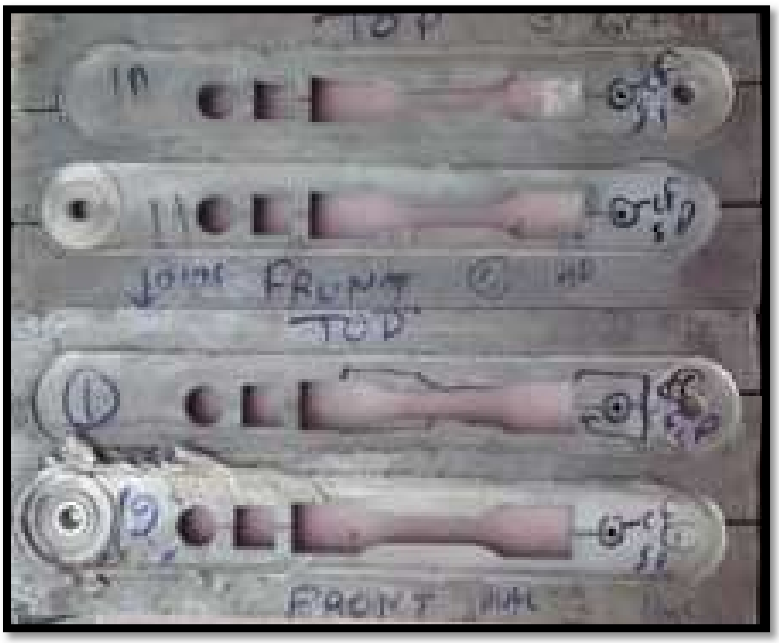

Fig. 4.3: Processed Plate after EDM wire cut.

Fig. 4.4: Specimen from Plate shown above via EDM wire cut. (a) Tensile specimen, (b) Hardness and microstructure specimen, (c) Wear test specimen.

Fig. 4.5: Specimen for Wear Test.

Chapter 5 RESULTS AND DISCUSSION

After conducting the experiments on four prepared samples using friction stir processing (FSP), the following observations have been made.

5.1 Hardness Test

5.1.1 Brinell Hardness Test

Observations:

HBS 5/750 (Hardness Ball Steel, 5mm diameter)

Force Applied (P) = 750 kgf

Diameter of Ball (D) = 5 mm

Time period for application of load =10 seconds

Table 5.1: Brinell Hardness Test Observations & Calculations

Test Sample	BHN Value
Base Metal	**86**
With no particles	**111**
With SiC	**116**
With SiC + B_4C	**120**
With B_4C	**129**

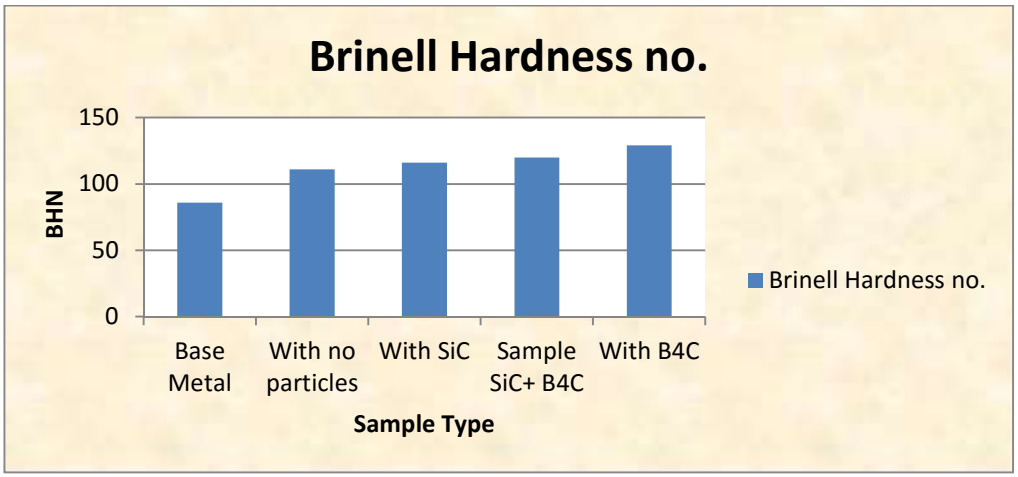

Fig. 5.1: Bar Graph representing Brinell Hardness No. of different samples

Inference:

a) Hardness value increases with FSP under 3 passes of tool even without any reinforced particles.

b) Hardness value further increases with the Silicon and boron Carbide addition as expected.

c) Highest value of hardness has been observed with B_4C, because boron carbide is very hard material as compared to silicon carbide and others.

5.1.2 Vickers Hardness Test

Observation:

Force Applied (P) = 100 gf

Dwell time of load =10 seconds

Table 5.2: Vickers Hardness Test Observations

Distance from the top surface (mm)	Base metal	With SiC	With B_4C	Sample SiC + B_4C	With no particles
0	95	128	142	133	122
1	95	126	139	129	119
2	95	122.5	137	113	116
3	95	114.5	130	120	115

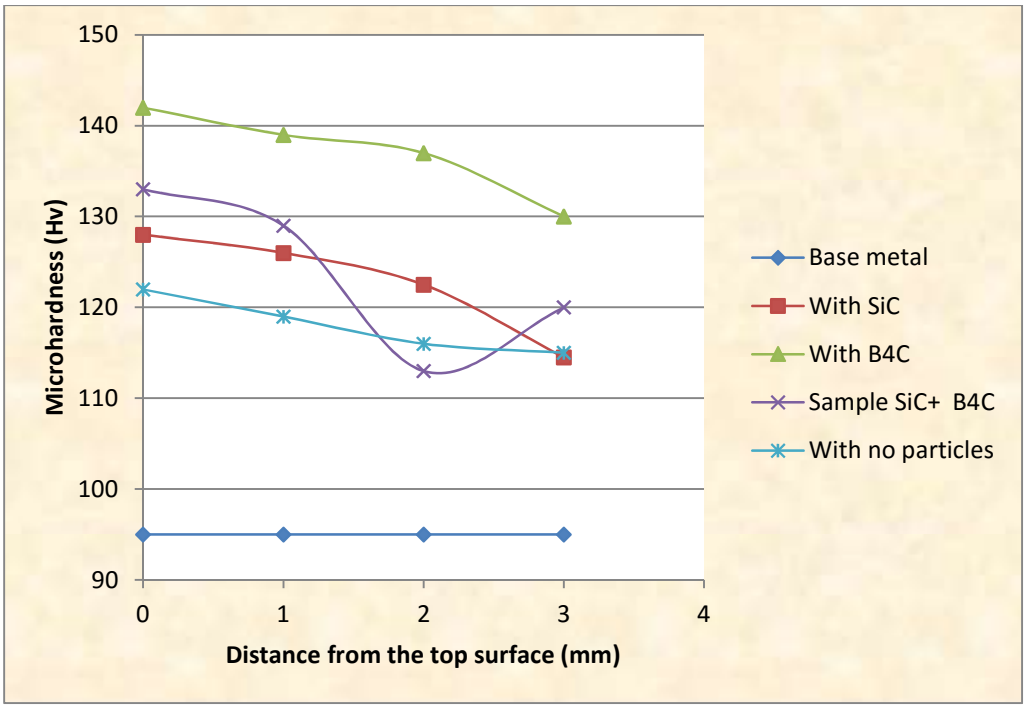

Fig. 5.2: Line Graph representing Vickers Hardness value of different samples

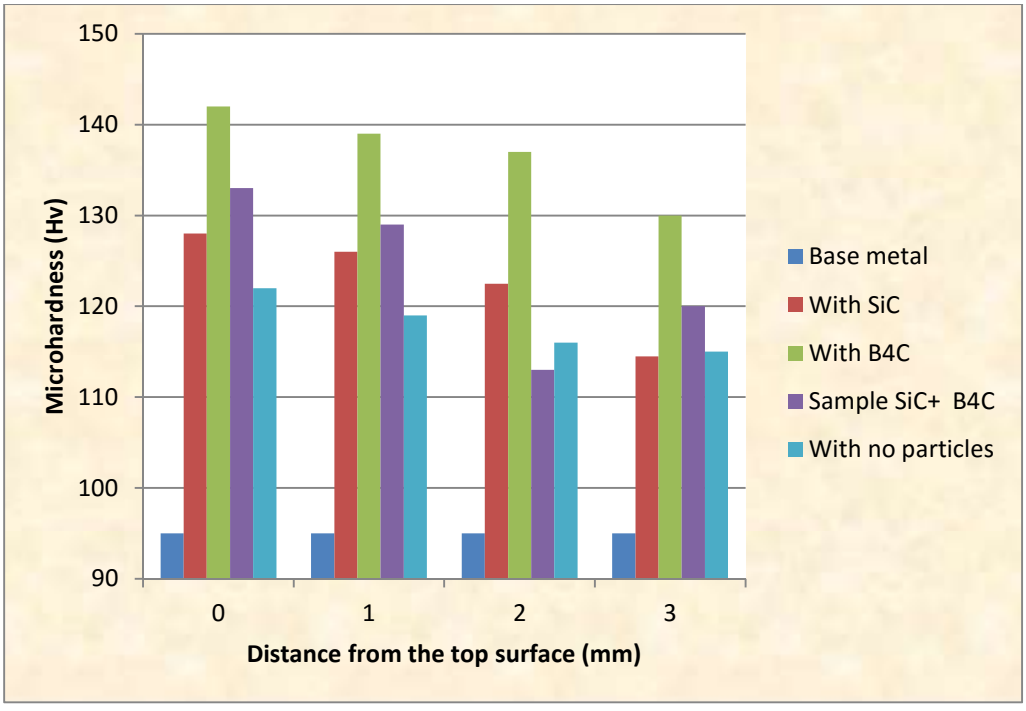

Fig. 5.3: Bar Graph representation of Vickers Hardness value for different samples

Inference:

a) Vickers Hardness value decrease as we go in depth of surface due to improper mixing in the depth

b) The surface composite layer (SCL) with boron carbide has shown better hardness value as compared to others.

c) The hardness is increased due to grain refinement of the particles and the higher hardness of the reinforced particles.

5.2 Wear Test

5.2.1 Weight loss and wear test

Table 5.3: Weight loss and wear rate at each interval of 500m (base material)**.**

Sliding Distance (m)	Wt. Loss (mg) (cumulative)	Wear Rate (mg/m) x 10^{-3}
500	3.4724	6.9448
1000	7.0594	7.0594
1500	10.4484	6.9656
2000	14.0712	7.0356
2500	17.3091	6.9236
3000	21.0008	7.0002
Coefficient of friction	**0.64**	**Avg. Wear Rate 6.9882**

Table 5.4: Weight loss and wear rate at each interval of 500 m (FSPed base material)

Sliding Distance (m)	Wt. Loss (mg) (cumulative)	Wear Rate (mg/m) x 10^{-3}
500	3.2568	6.5136
1000	6.5124	6.5124
1500	9.8684	6.5122
2000	12.8912	6.4956
2500	16.4071	6.5228
3000	19.5908	6.5302
Coefficient of friction	**0.61**	**Avg. Wear Rate 6.5144**

Table 5.5: Weight loss and wear rate at each interval of 500 m (FSPed with SiC)

Sliding Distance (m)	Wt. Loss (mg) (cumulative)	Wear Rate (mg/m) x 10^{-3}
500	2.9052	5.8104
1000	5.6458	5.6458
1500	8.3618	5.5744
2000	11.2769	5.6384
2500	13.7618	5.5047
3000	16.5589	5.5202
Coefficient of friction	**0.55**	**Avg. Wear Rate 5.6157**

Table 5.6: Weight loss and wear rate at each interval of 500 m (FSPed with $SiC+B_4C$)

Sliding Distance (m)	Wt. Loss (mg) (cumulative)	Wear Rate (mg/m) x 10^{-3}
500	2.2522	4.5044
1000	4.5262	4.5262
1500	6.8487	4.5658
2000	9.0152	4.5076
2500	11.2957	4.5182
3000	13.5972	4.5324
Coefficient of friction	**0.48**	**Avg. Wear Rate 4.5258**

Table 5.7: Weight loss and wear rate at each interval of 500m (FSPed with B_4C)

Sliding Distance (m)	Wt. Loss (mg) (cumulative)	Wear Rate (mg/m) x 10^{-3}
500	1.385	2.77
1000	2.782	2.782
1500	4.1425	2.7616
2000	5.543	2.7715
2500	6.749	2.6996
3000	8.372	2.7907
Coefficient of friction	**0.41**	**Avg. Wear Rate 2.7625**

5.2.2 Graphs

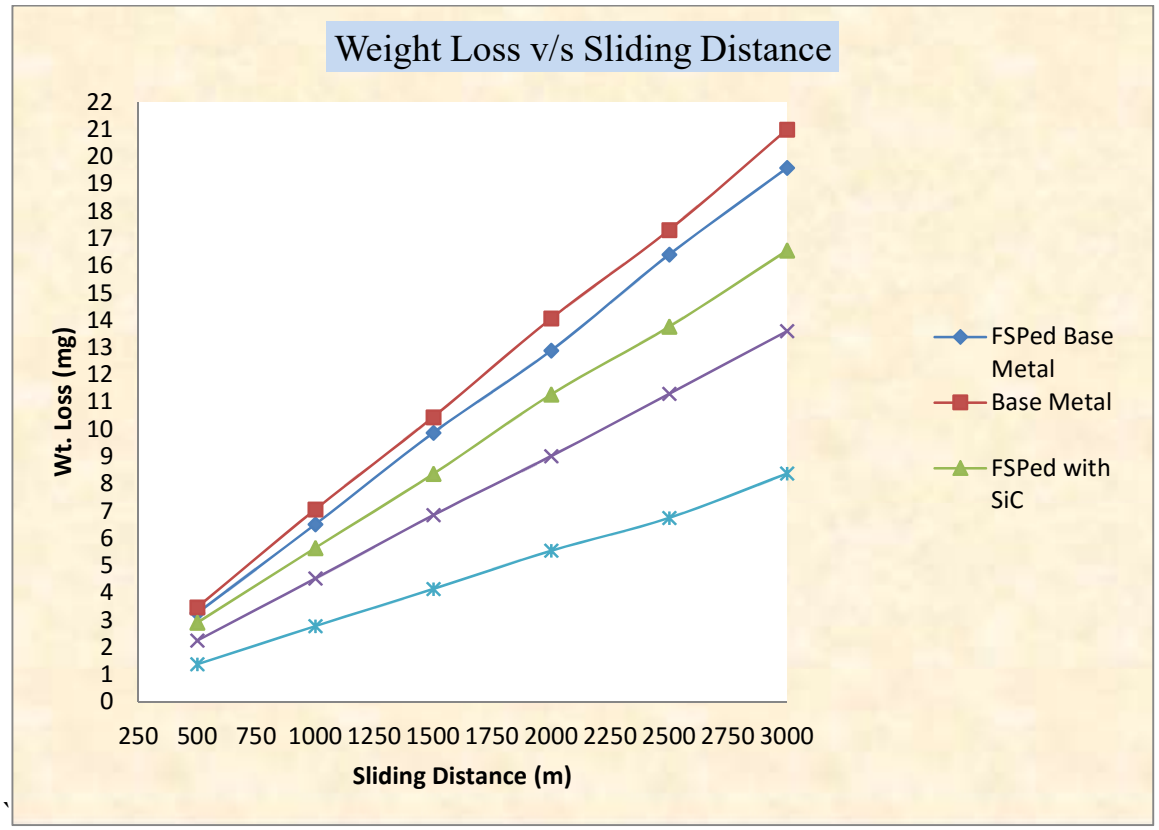

Fig. 5.4: Graph between Sliding distance and weight loss for various samples

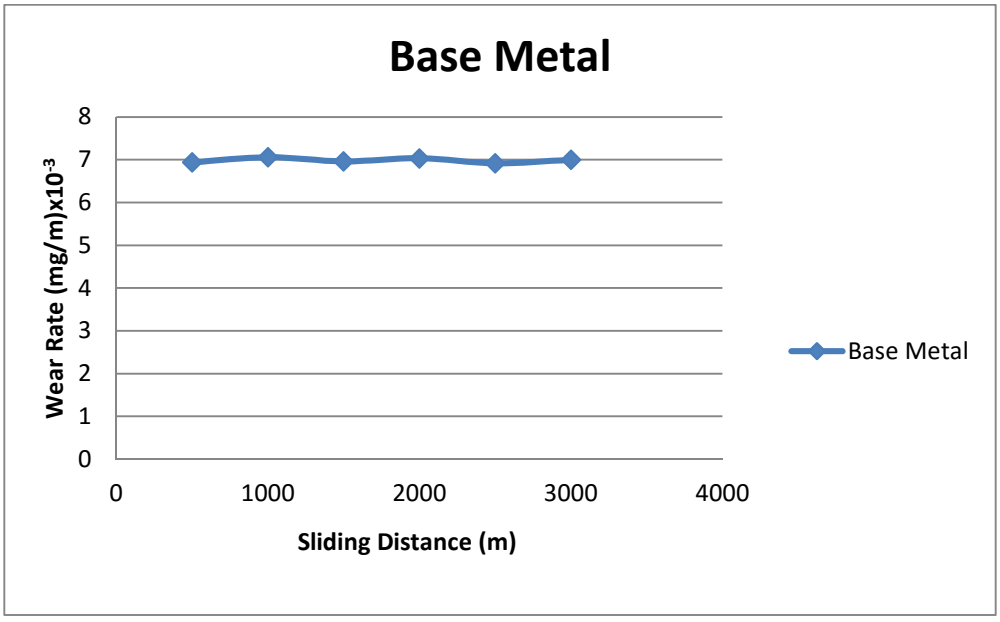

Fig. 5.5: Graph between Wear rate and sliding distance for base metal

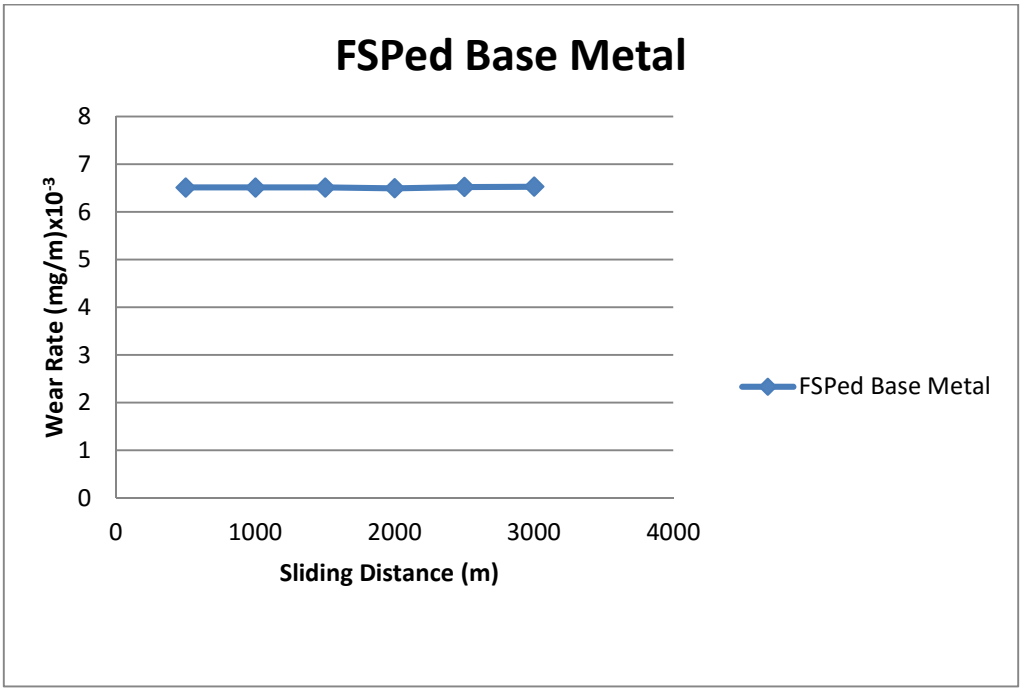

Fig. 5.6: Graph between Wear rate and sliding distance for FSPed base metal

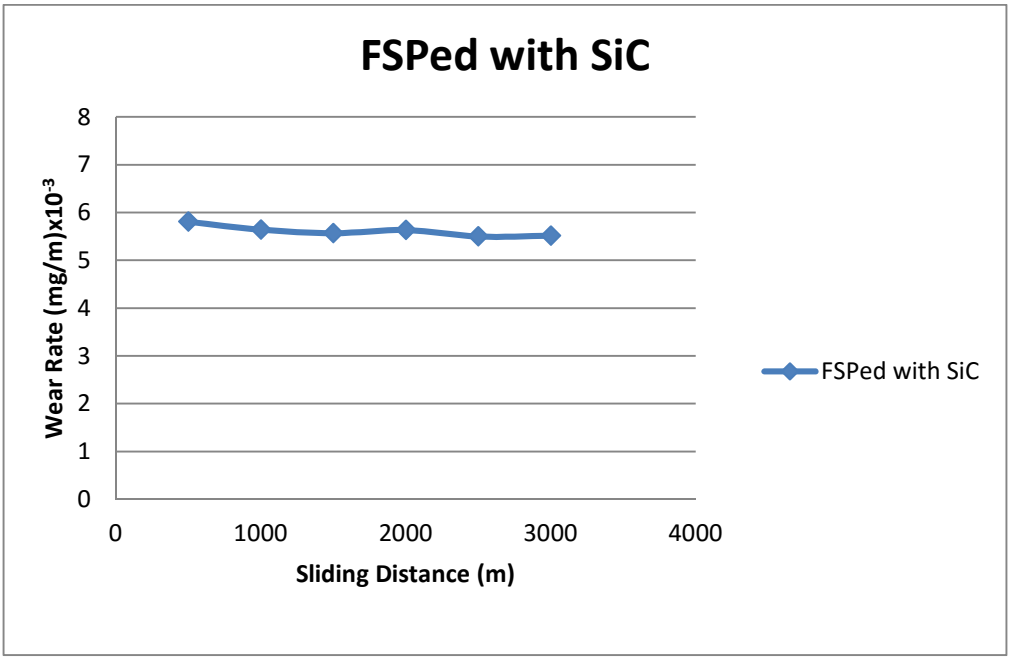

Fig. 5.7: Graph between Wear rate and sliding distance for FSPed with SiC

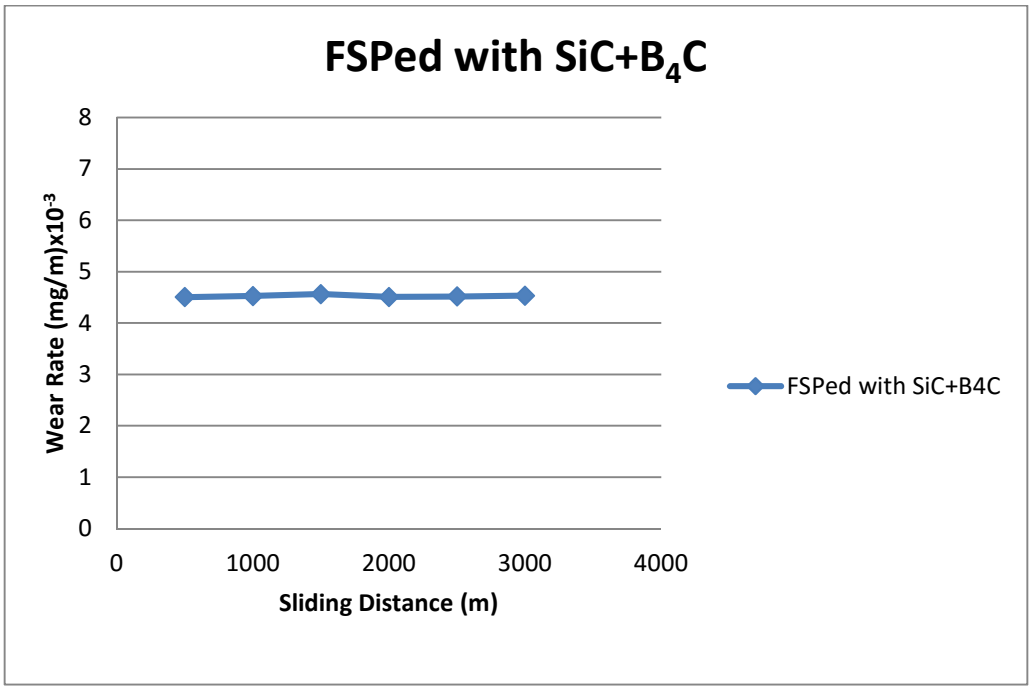

Fig. 5.8**:** Graph between Wear rate and sliding distance for FSPed with SiC+B_4C

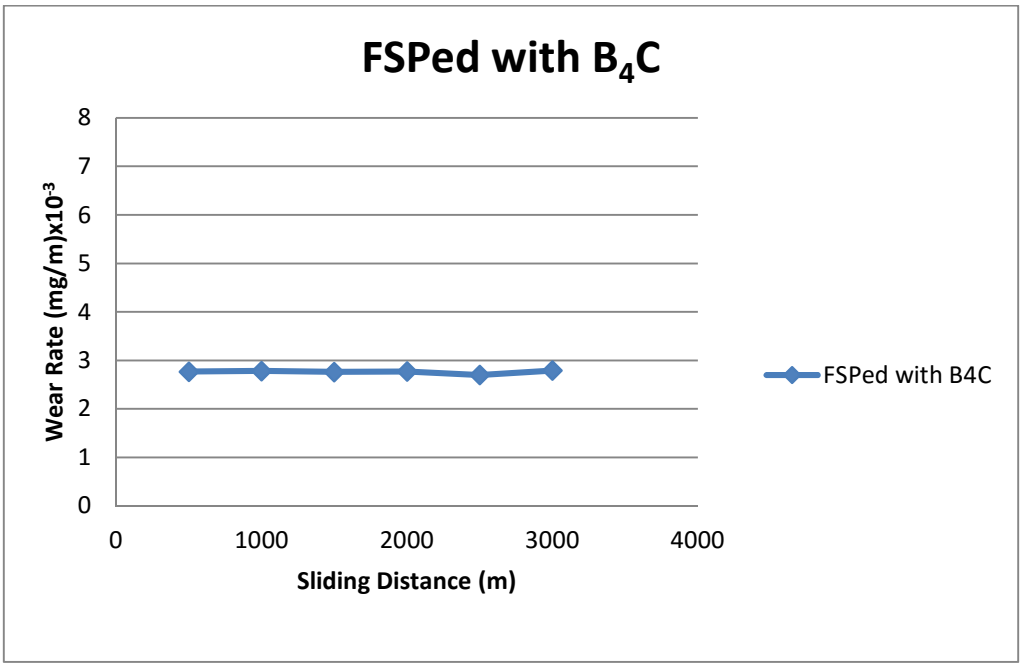

Fig. 5.9: Graph between Wear rate and sliding distance for FSPed with B_4C

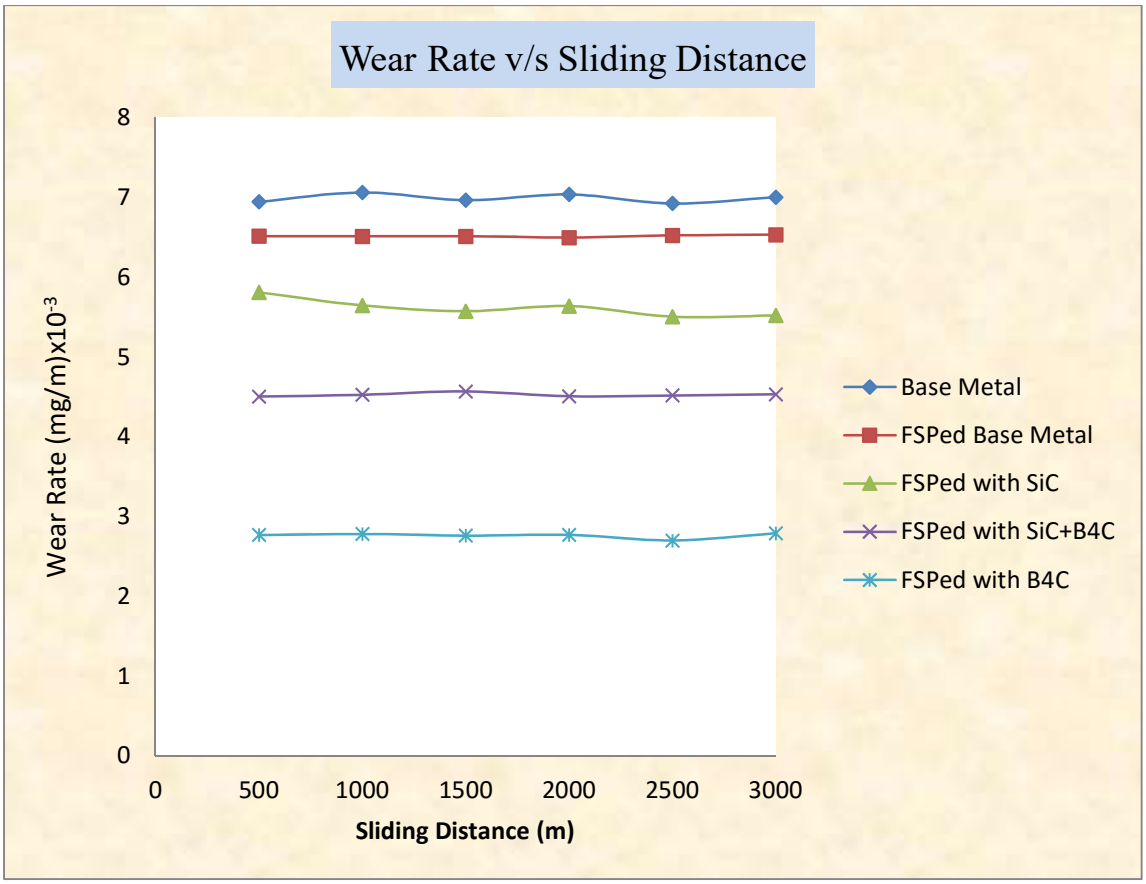

Fig. 5.10**:** Line Graph representing comparison between wear rate and sliding distance for all the sample

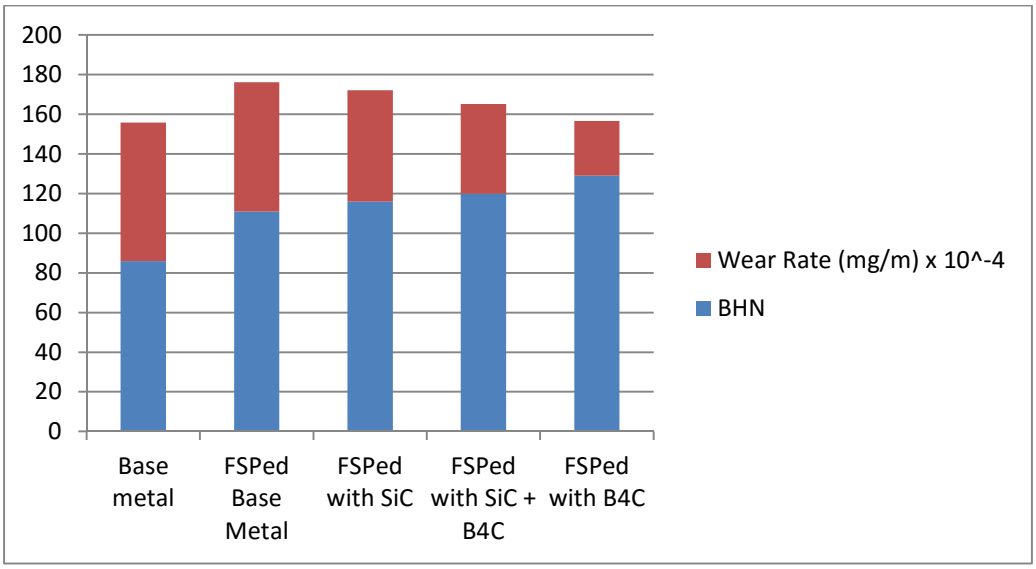

Fig. 5.11**:** Graph representing Hardness and wear rate values variation for all samples

***Inference*:**

- The surface composite layer (SCL) with boron carbide has shown best wear resistant properties among all samples.
- It has also been observed that as hardness value increases, wear rate decreases and hence, weight loss decreases.
- From fig. 4.16, it has been observed that the relation between hardness and wear rate are found as inversely proportional.
- Decrease in wear rare is also observed due to the reduced grain size i.e., fine microstructure.

5.3 Tensile Test

Observation:

Table 5.8: Tensile Strength Test Observation

Test Sample	Width (mm)	Thickness (mm)	Area (mm^2)	Gauge Length (Initial) (mm)	Gauge Length (Final) (mm)	Ultimate Force (N)	Ultimate Stress (MPa)
Base Metal	7	6.12	42.84	35	**42.9**	**6500**	**155**
FSPed Base Metal	6	3.97	23.82	20	**22.51**	**5000**	**208**
FSPed with SiC	6	4.00	24	20	**21.6**	**2730**	**114**
FSPed with SiC+B_4C	6	4.03	24.18	20	**22.48**	**5110**	**213**
FSPed with B_4C	6	4.12	24.72	20	**22.32**	**5970**	**249**

Calculation and Result:

Table 5.9: Tensile Strength Test Calculation

Test Sample	Observed Ultimate Stress (MPa) (A)	Corrected Ultimate Stress (MPa) = Force/Corrected area	Elongation Percentage (%)
Base Metal	**155**	**152**	**22.57**
FSPed Base Metal	**208**	**210**	**12.55**
FSPed with SiC	**114**	**114**	**8.33**
FSPed with SiC+B_4C	**213**	**212**	**12.40**
FSPed with B_4C	**249**	**242**	**11.60**

Graphs (Stress- Strain and Force- Displacement):

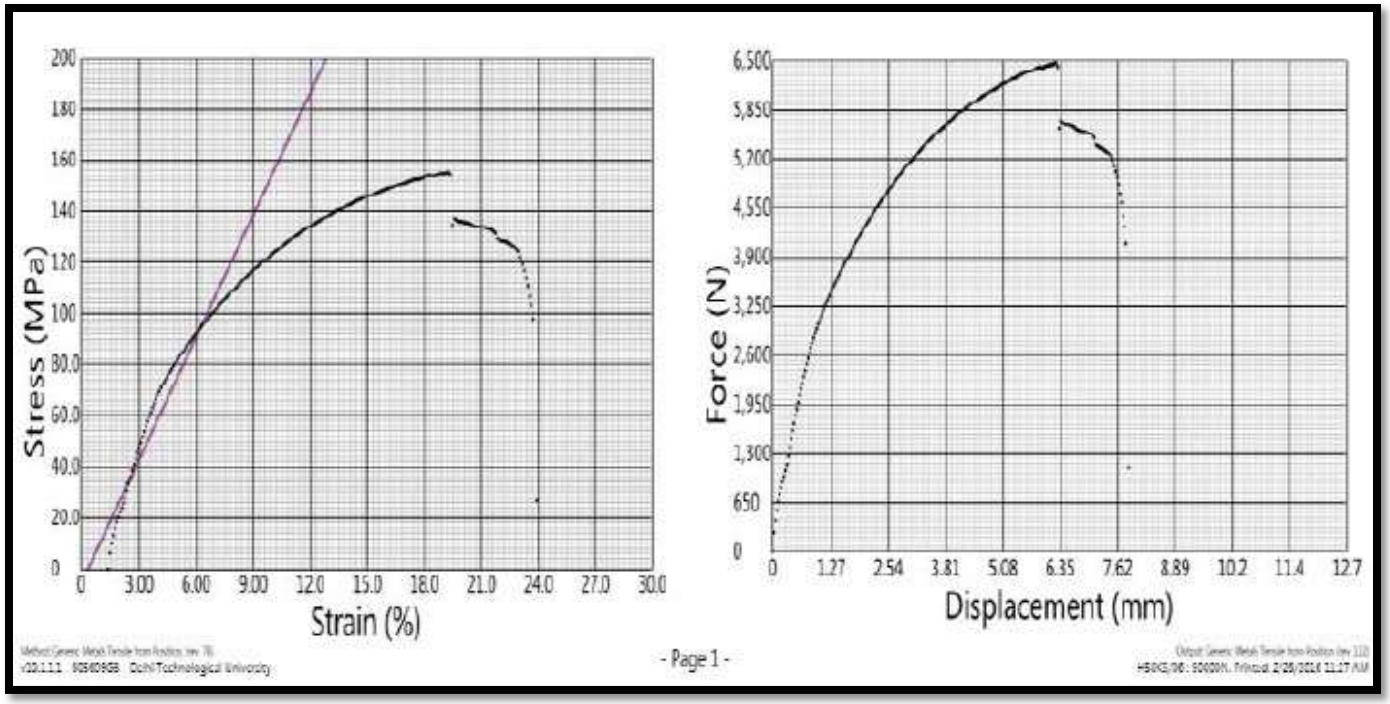

Fig. 5.12: Base Metal Stress-Strain & Force-Displacement

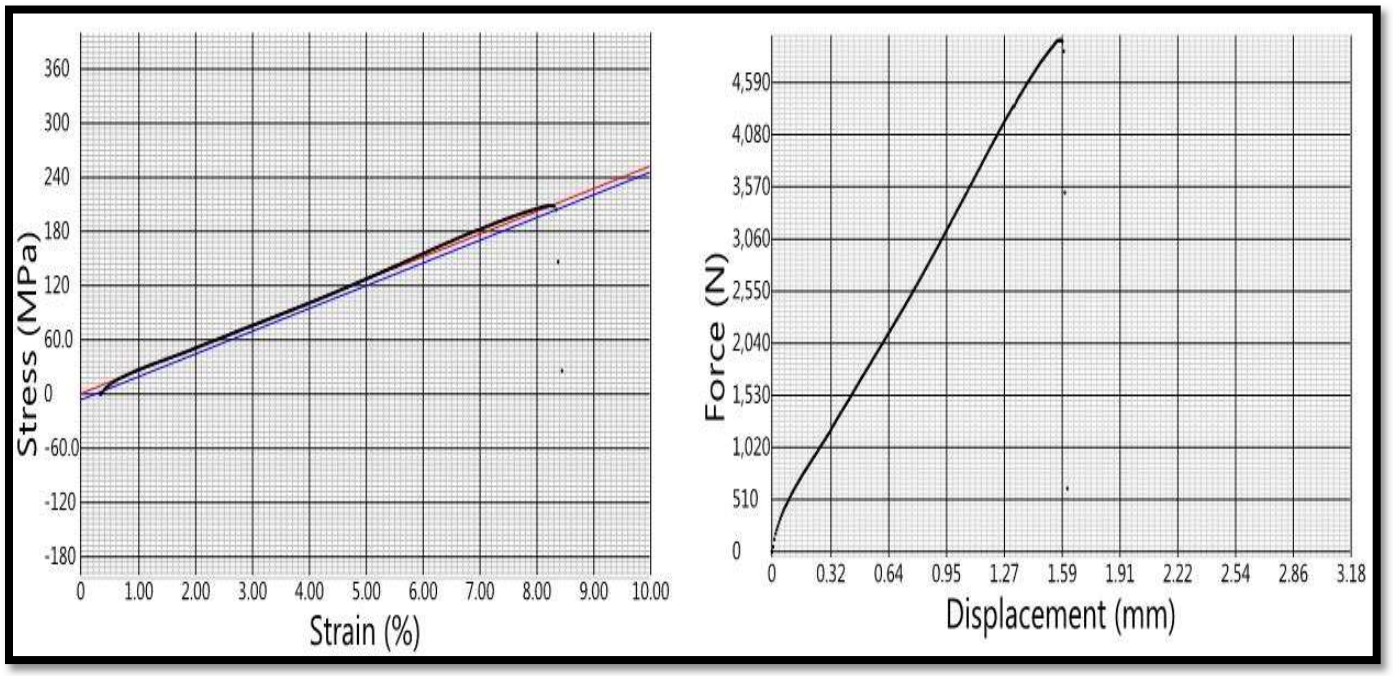

Fig. 5.13: FSPed Base Metal Stress-Strain & Force-Displacement

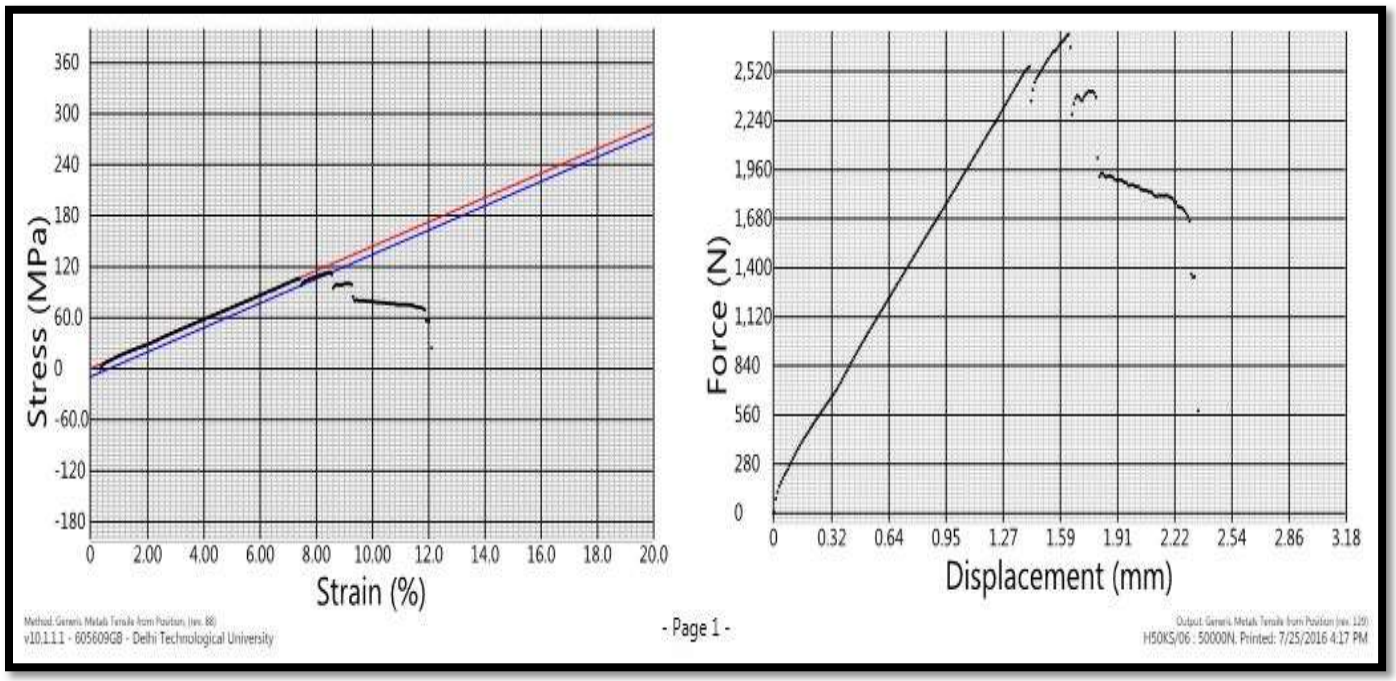

Fig. 5.14: FSPed with SiC Stress-Strain & Force-Displacement

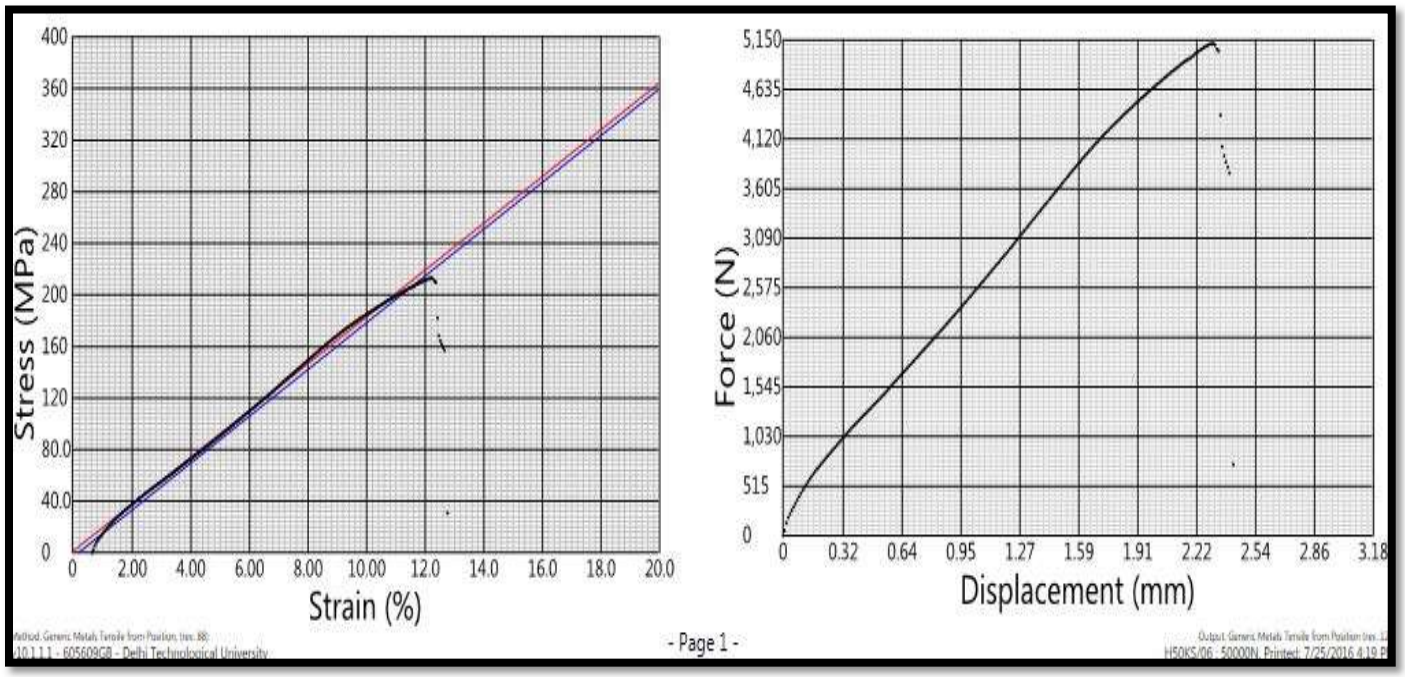

Fig. 5.15: FSPed with SiC + B_4C Stress-Strain & Force-Displacement

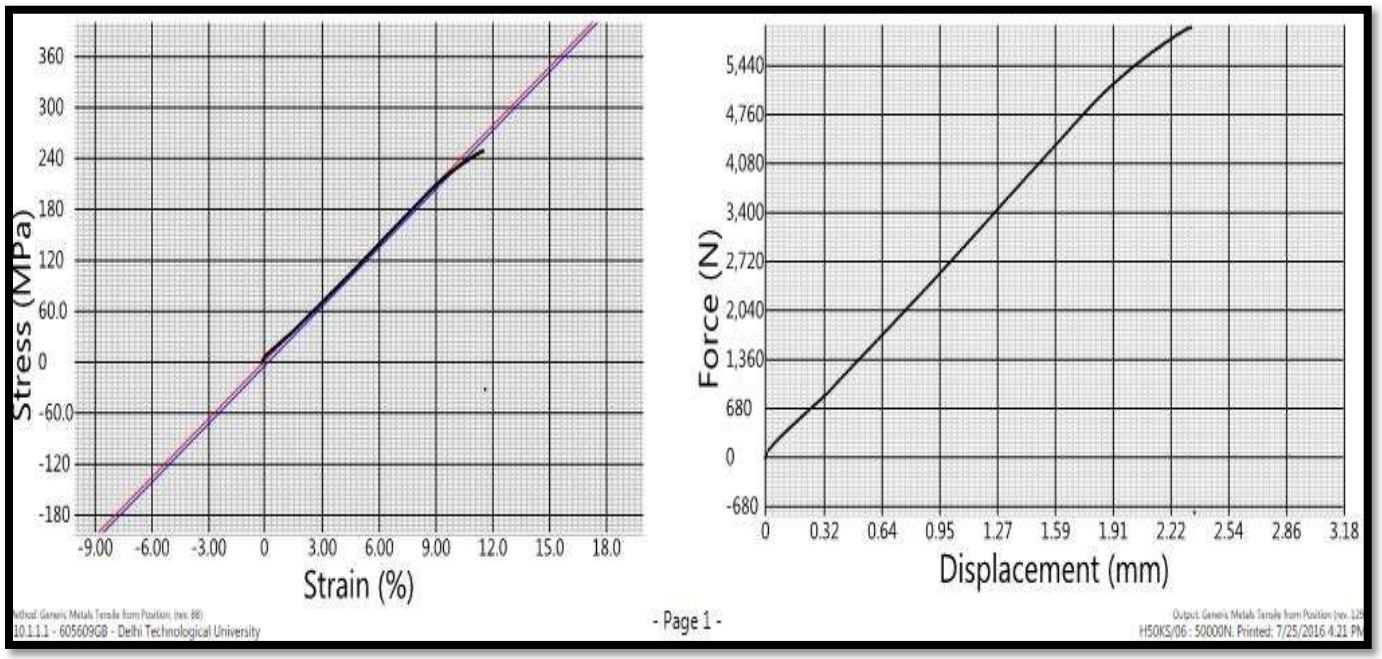

Fig. 5.16: FSPed with B_4C Stress-Strain & Force-Displacement

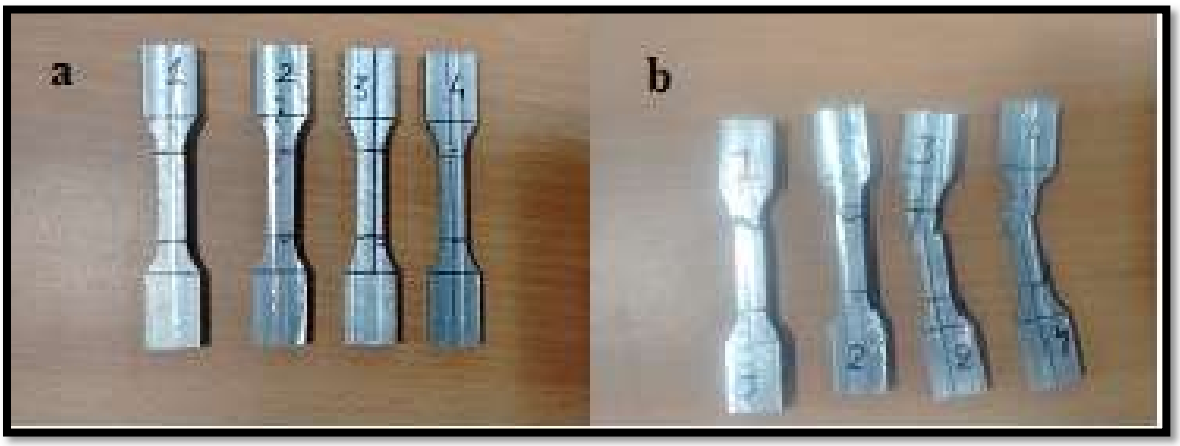

Fig. 5.17: Tensile specimen a) Before Testing b) After Testing

Inference:

- UTS of sample processed with SiC reduces drastically due to porosity formation in SCL. Reason behind that would be:
  - Blow holes
  - Air Trap
  - Pin holes
  - Scales on work-piece surfaces
- Rest all sample's UTS increases with increase in a hardness of reinforced particle. And hence, elongation decreases.

5.4 Microstructure Analysis

As per all the test results, FSPed with Boron Carbide has shown best results in terms of wear resistant, hardness value, and Tensile strength. We have done microstructure analysis only for the sample which is FSPed with Boron Carbide (B_4C) as reinforced particle.

Microstructure Observed:

Fig. 5.18: Microstructure Analysis using optical microscopy

Inference:

- From fig. 5.18, it has been observed that the boron carbide particles are distributed uniformly.
- It shows the fine grain structure
- Microstructure proves the reason behind the best hardness, wear resistance and tensile strength for B_4C reinforced particles among all samples.

5.5 Scanning Electron Microscopy Test

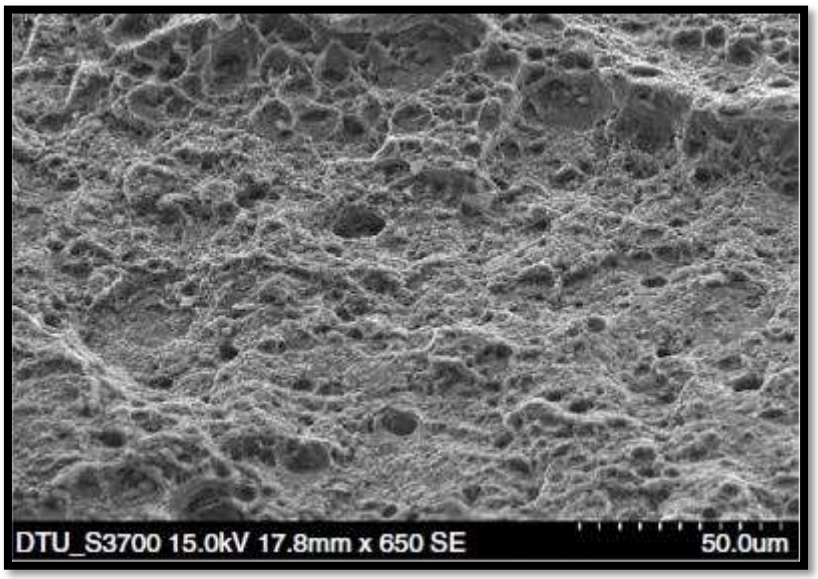

Fig. 5.19: SEM analysis for the FSPed Specimen with Boron Carbide

Inference:

- Boron Carbide distributed uniformly on the surface plate after the 3 passes of tool movement over the plate.
- Identifying the B_4C particles in the matrix is difficult due to its small molecular structure and size of the particles used.

Chapter 6 CONCLUSIONS AND SCOPE FOR FUTURE WORK

6.1 Conclusion

Friction stir processing (FSP) is a new grain refinement and micro structural modification techniques based on severe plastic deformation (SPD). The FSP is the best technique among like equal-channel angular pressing/extrusion (ECAP/E), high pressure torsion (HPT), and accumulative roll-bonding (ARB) as considering the processing of large-scale plate or sheet-type materials. Friction stir processing has immensely high potential in the field of thermo mechanical processing of various alloys especially the aluminium alloys. In the present research work we successfully processed the surface of AA6061 T6 aluminium alloy at 1000 rpm and 25mm/min with cylindrical threaded pin profile tool of M35 HSS tool material with fixed number of passes (i.e. 3) and studied the microstructure, tensile properties, and micro-hardness and wear behavior of FSPed surface of aluminium alloy with different reinforced particles and compared with the properties of base material. We used Silicon carbide, Boron Carbide and mixture of both in equal volume percentage as different reinforced particles. So we fabricated the reinforced surface composite which was successfully tested.

This chapter summarize all the major observations and the conclusions drawn from this study as well as highlights the significant contributions of this thesis to the existing knowledge. And it also summarizes the future scope of work.

1. The hardness of Friction stir processed samples (FSPed) has been found increased with the use of harder reinforced particles (B_4C) as compared to other reinforeced particles as well as without reinforced particles.
2. The micro-hardness of FSPed with B_4C sample (137 Hv) has been observed higher as compared to FSPed with SiC reinforced particles (122.75 Hv) and FSPed without reinforced particle (118 Hv) of 6061 T6 aluminium alloy.
3. It has been observed that the wear rate of friction stir processed samples has been found minimum with harder reinforced particles (B_4C) for same sliding distance 3000 meter and constant speed 382 rpm as compared to all other samples.
4. The average coefficient of friction has been observed minimum with B_4C reinforced particles for same loading 40N among all other samples.

5. The ultimate tensile strength (210MPa) of FSPed base material sample is higher as compared to base material (152MPa). The ultimate tensile strength of FSPed sample with reinforced particle B_4C has been found maximum among all other sample.
6. The ultimate tensile strength (114 MPa) and elongation (8.33%) of FSPed with SiC sample has been found reduced drastically due to the formation of the porosity during processing. Necking being observed from only that area which has become weak due to the porosity.
7. The percentage elongations for processed samples are on base metal (22.57%), FSPed with base metal (12.57%), FSPed with SiC (8.33%), FSPed with SiC + B_4C (12.40%)and FSPed with B_4C (11. 60%).With increasing hardness of reinforced particles the percentage tensile elongation is decreased as compared to base material (22.57%) samples.

6.2 Future Scope of Work

Further Investigation on Al 6061 can also be done by varying following parameters also.

- Tool pin design
- Different No. of Passes
- Different dimension of slot
- Different axial load
- Feed rate
- Tool tilt angle

References

1. Thomas, W.M., Nicholas, E.D. and Kallee, S.W., "Friction based technologies for joining and processing", Friction Stir Welding and Processing, Edited by K.V. Jata, M.W. Mahoney, R.S. Mishra, S.L. Semiatin, and D.P. Field, TMS, 2001, Pages 3-13.
2. Powell, H.J. and Wiemer, K., "Joining technology for high volume manufacturing of lightweight vehicle structures", Article ,1996, TWI, Cambridge, UK.
3. Thomas, W.M. and Nicholas, E.D., "Friction stir welding for the transportation industries. Materials & Design", 1997 Volume 18, 269-273.
4. Mishra, R.S and Mahoney, M.W, "Friction Stir Processing: A New Grain Refinement Technique in Commercial Alloys", Materials Science Forum, 2001, Volumes357-359, Pages 507-514.
5. R. S. Mishra, Z. Y. Ma and I. Charit, "Friction stir processing: a novel technique for fabrication of surface composite", Materials Science and Engineering A, Volume 341, Issues 1-2, 20 January 2003, Pages 307-310.
6. Thomas, W.M., Nicholas, and E.D., 1996. Emerging friction stir joining technology for stainless steel and aluminium applications, presented at 'Productivity beyond 2000': IIW Asian pacific Welding Congress, Auckland, New Zealand.
7. M. Peel, A. Steuwer, M. Preuss and P. J. Withers, "Microstructure, mechanical properties residual stresses as a function of welding speed in aluminium AA5083 friction stir welds", Acta Materialia, Volume 51, Issue 16, 2003, Pages 4791-4801.
8. C. G. Rhodes, M. W. Mahoney, W. H. Bingel and M. Calabrese, "Fine-grain evolution in friction-stir processed 7050 aluminums", Scripta Materialia, Volume 48, Issue 10, May 2003, Pages 1451-1455.
9. Y. S. Sato, Y. Kurihara, S. H. C. Park, H. Kokawa and N. Tsuji , "Friction stir welding of ultrafine grained Al alloy 1100 produced by accumulative roll-bonding", Scripta Materialia, Volume 50, Issue 1, 2004, Pages 57-60.
10. M. Cabibbo, E. Meccia and E. Evangelista , "TEM analysis of a friction stir-welded butt joint of Al–Si–Mg alloys", Materials Chemistry and Physics, Volume 81, Issues 2-3, 28 August 2003, Pages 289-292.

11. L. Lity ska, R. Braun, G. Staniek, C. Dalle Donne and J. Dutkiewicz , "TEM study of the microstructure evolution in a friction stir-welded AlCuMgAg alloy", Materials Chemistry and Physics, Volume 81, Issues 2-3, 28 August 2003, Pages 293-295.
12. J. Q. Su, T. W. Nelson, R. Mishra and M. Mahoney , "Microstructural investigation of friction stir welded 7050-T651 aluminium", Acta Materialia, Volume 51, Issue 3, 7 February 2003, Pages 713-729.
13. Y. J. Kwon, I. Shigematsu and N. Saito, "Mechanical properties of fine-grained aluminum alloy produced by friction stir process", Scripta Materialia, Volume 49, Issue 8, October 2003, Pages 785-789.
14. Berbon, P.B., Bingel, W.H., Mishra, R.S., Bampton, C.C., Mahoney and M.W.,. "Friction stir processing: a tool to homogenize nanocomposite aluminum alloys" Scripta Materialia Volume 44, Issue: 1, 2001, Pages 61-66.
15. Devaraju Aruri, Kumar Adepu, Kumaraswamy Adepu, Kotiveerachari Bazavada, "Wear and mechanical properties of 6061-T6 aluminum alloy surface hybrid composites [(SiC + Gr) and (SiC + Al_2O_3)] fabricated by friction stir processing", Journals of material research and technology 2013;362-369.
16. Narayana Yuvaraj, Sivanandam Aravindan, Vipin Fabrication of Al5083/B4C surface composite by friction stir processing and its tribological characterization", Journals of material research and technology,. 18 march, 2015,398-410.
17. http://www.azom.com/article.aspx?ArticleID=2863
18. Wanchuck Woo, Hahn Choo, Donald W. Brown, and Zhili Feng, "Influence of the Tool Pin and Shoulder on Microstructure and Natural Aging Kinetics in a Friction-Stir-Processed 6061 – T6 Aluminium Alloy", The Minerals, Metals & Materials Society and ASM International, 2007, 152 -161.
19. B. Zahmatkesh, M. H. Enayati, F. Karimzadeh, "Tribological and microstructural evaluation of friction stir processed Al2024 alloy", Materials and Design. 31, 2010, 4891–4896.
20. Chandan Deep Singh, Ripandeep Singh, Naveen Kumar "Effect of FSP Multipass on Microstructure and Impact Strength of AL6063", American International Journal of Research in Science, Technology, Engineering & Mathematics, march 2014 Pp. 140-145.

21. Kim Y. G, Fujii H., Tsumura T., Komazaki T., Nakata K. “Effect of welding parameters on microstructure in the stir zone of FSW joints of aluminum die casting alloy”, Materials Letters, 2006, 60(29−30), 3830−3837.
22. Kumar K., Satish V Kailas, “On the role of axial load and the effect of interface position on the tensile strength of a friction stir welded aluminium alloy”, Journals of Materials and Design, 2008, 29(4): 791−797.
23. Ouyang J. H., Kovacevic R. “Material flow during friction stir welding (FSW) of the same and dissimilar aluminum alloys”, Journal of Material Engineering and Performance, 2002, 11(1) 51−63.
24. Krishnan K. N., “On the formation of onion rings in friction stir welds”, Journal of Materials Science and Engineering A, 2002, 327(2): 246−251.
25. ASTM International, "Standard Test Methods for Rockwell Hardness of Metallic Materials", ASTM E18-15, http://www.astm.org/Standards/E18.htm, accessed February 2016.
26. ISO, "Metallic materials - Brinell hardness Test-Part 1: Test method", ISO 6506-1:2014, http://www.iso.org/isocatalogue_detail.htm?csnumber=59671, accessed February 2016
27. http://www.gordonengland.co.uk/hardness/vickers.htm.
28. ISO, "Metallic Materials-Tensile Testing-Part 1: Method of test at room temperature", ISO 6892-1:2009, http://www.iso.org/iso/catalogue_detail.htm?csnumber=51081, accessed February 2016.
29. ASTM International, "Standard Test Methods for Tension Testing of Metallic Materials", ASTM E8 / E8M-15a, http://www.astm.org/Standards/E8.htm, accessed February 2016
30. SEM Setup, http://medicine.utoronto.ca/sites/default/files/SEM_2015.jpg, accessed February 2016.
31. SEM Manual, https://imf.ucmerced.edu/downloads/semmanual.pdf, accessed February 2016.
32. www.astmsteel.com/product/tool-steel-M35-1-3243-hs6-5-2-5-skh55/
33. S. Jerome, S. Govind Bhalchandra, S.P. Kumaresh Babu, B. Ravisankar, 2012, Influence of Microstructure and Experimental Parameters on Mechanical and Wear Properties of Al-TiC Surface Composite by FSP Route, Journal of Minerals & Materials Characterization & Engineering, **11(5)**, 493-507.

34. http://www.azom.com/article.aspx?ArticleID=75